Journal Pre-proof

Modeling risk contagion in the Italian zonal electricity market

Emmanuel Senyo Fianu, Daniel Felix Ahelegbey, Luigi Grossi

PII: S0377-2217(21)00568-3
DOI: https://doi.org/10.1016/j.ejor.2021.06.052
Reference: EOR 17317

To appear in: *European Journal of Operational Research*

Received date: 18 December 2019
Accepted date: 23 June 2021

Please cite this article as: Emmanuel Senyo Fianu, Daniel Felix Ahelegbey, Luigi Grossi, Modeling risk contagion in the Italian zonal electricity market, *European Journal of Operational Research* (2021), doi: https://doi.org/10.1016/j.ejor.2021.06.052

Highlights

- Network models enhance the efficient analysis of electricity market connections.
- Intra-day and inter-day electricity market zones interconnections are estimated.
- Evaluation of dynamics and persistence of zonal links in the Italian market.
- Identification of physical zones that play a dominant role in the spread of risk.
- Useful support to policymakers in decisions concerning the transmission grid.

Title page

Modeling risk contagion in the Italian zonal electricity market

Emmanuel Senyo Fianu[a], Daniel Felix Ahelegbey[b], Luigi Grossi[c,*]

[a] *Leuphana University of Lüneburg, Universitätallee 1, 21335 Lüneburg, Germany and Mainz University of Applied Sciences, Mainz, Lucy-Hillebrand-Str. 2, 55128, Mainz, Germany* emmanuelsenyo.fianu@gmail.com; *and* emmanuel.fianu@hs-mainz.de

[b] *Boston University, Department of Mathematics and Statistics, 111 Cummington Street, Boston, MA 02215, USA -* dfkahey@bu.edu

[c] *University of Verona, Department of Economics, Via Cantarane 24, 37129 Verona, Italy -* luigi.grossi@univr.it

*Corresponding author

Email addresses: emmanuelsenyo.fianu@gmail.com and emmanuel.fianu@hs-mainz.de (Emmanuel Senyo Fianu), dfkahey@bu.edu (Daniel Felix Ahelegbey), luigi.grossi@univr.it (Luigi Grossi)

Abstract

Ensuring the security of stable, efficient and reliable energy supplies has intensified the interconnections between energy markets. Imbalances between supply and demand due to operational failures, congestion and other sources of risk faced by market connections can lead to a system that is vulnerable to the spread of risk and its spill-over. The main contribution of this paper is the development and estimation of a Bayesian Graphical Vector-AutoRegression and a Bayesian Graphical Structural Equation Modelling with external regressors - BG-VARX and BG-SEMX, respectively - enhancing the proper analysis of market connections.

The Italian electricity market has been chosen because it is a clear example of a zonal market where risk can spread over connected zones. We estimate, for the first time, within-day and across-day zonal market interconnections with a multivariate time series of hourly prices, actual and forecast power demand and forecast wind generation over the period 2014-2019 and evaluate the dynamics and persistence of zonal market connections, examining the spread of risk in the zones of the Italian electricity market.

Our findings provide an improved, accurate explanation of risk contagion, identifying the zones that are most influential in terms of hub centrality (major transmitters) and authority centrality (major recipients), respectively, for intra-day and inter-day risk propagation in the Italian electricity market. In addition, the policy implications in terms of market-monitoring are discussed.

Keywords

OR in energy; complex networks; electricity price volatility; systemic risk; zonal electricity market

JEL: C11; C15; C32; C52; G01; Q41

1. Introduction

For several decades, in many countries, the hallmark of energy policy and regulation has been security in energy supply and its reliability. Recently, the focus of the energy sector has been on improving economic efficiency, increasing productivity and reducing costs, thereby providing long-term efficiency gains. Specifically, in the electricity sector, many markets have introduced competitive bid-based electricity auctions to set energy prices and capacity, which often involve congestion costs (Creti and Fontini, 2019). Several of the efficiency mechanisms put in place are facing new and unexpected challenges in terms of transmission and distribution.

In this research we exploit the structure of the Italian electricity market as a unique case study for the understanding of the interconnections in a zonal market and the results of the study may help to examine risk propagation in the zones in which the market is organized. Moreover, the benefit of various regulatory and structural changes in the zonal electricity market can be calculated in full, accounting for volatility interconnections between zones.

This paper studies the relationships governing the risk spread over the zones of the Italian electricity market, and seeks to understand the impact of market integration, resulting from new interconnections and other structural changes. Many causes underlie the exposure of the Italian electricity market to risks of contagion between zones (see, for instance, Creti et al.,

2010). The efficiency of zonal pricing is challenged by its failure, in network management, to take into account the behavioral perspective of the public good, because of the indivisibility of network security. In addition, it neglects consumer behavior in terms of price differentials, which impact on overall social welfare. Evidently, enhancing welfare from the viewpoint of new interconnections is only beneficial to the region that starts off with higher prices (see, for instance, Creti et al., 2010) i.e Sardinia and Sicily.

However, de Menezes and Houllier (2015) examine potential implications of national policies and their impact on the electricity mix for interconnected European electricity markets and point out that the physical interconnections between European markets signal a trade-off between lower average prices and the export of volatility from larger markets with richer endowments of intermittent renewable sources. As such, it involves higher risk, which may prevent new investments in power generating facilities.

Despite the different methods adopted in pricing electricity, various network structures inherent in the market need to be explored and these provide the first steps in understanding the extent of risk exposure in the market (Zugno and Conejo, 2015). Congestions in transmission lines cause price differences in various zones of the network (Fianu, 2015).

Sapio and Spagnolo (2020) examine transmission volatility patterns via the VAR-GARCH estimation approach, before and after the inauguration of a new cable infrastructure, accounting for linkages in electricity market zones rich in intermittent renewable energy sources. As indicated by Klos et al. (2015), the configuration of the zonal energy market is often a result of political decisions. Among the methods developed to aid zonal delimitation, Klos et al. (2015) present a technique which aims to curb the loop flow effect, an element of unscheduled flows that introduces a loss of market efficiency in addition to a detailed decomposition of power flow in order to carry out zonal partitioning and to identify zones which cause problems in the network. Our approach contributes to this strand of literature because it identifies changes in the dynamics of volatility contagion both in terms of the originating source and of the "path" followed by the shocks in their spread across the geographical zones of an electricity market.

In detail, the original contributions of this paper can be summarized as follows. First, to the best of our knowledge, no paper has put forward and developed BG-VARX and BG-SEMX and further considered their applications, specifically, to examine the spread of systemic risk in zonal electricity markets. Our paper, therefore, presents these frontier methodologies in studying energy markets as built up on the Bayesian Graphical Vector Autoregression (BG-VAR) model by Ahelegbey et al. (2016a). The procedure suggested in this paper aims at correctly identifying the network structure risk inherent in the Italian electricity market. This is interesting for various reasons. The volatility dynamics and patterns can be used to understand deregulation, structural transformation and other regulatory processes and may explain competition in the electricity markets in relation to spot and future prices. In addition, a good model identification is essential for proper network congestion management in the quest for continuous real-time balancing and the need for forecasting, trading, generation planning, plant availability and for risk management purposes, among others. Since transmission pricing provides economic signals, which can lead to the efficient use of transmission grids, this paper provides an accurate indication of such signals by tracing the "path" of shocks and thus can help capture most of the economic benefits of efficient congestion management.

Another original contribution of this paper is the introduction of two different types of analysis of risk contagion: "intra-day" and "inter-day". The intra-day mechanism spreading volatility refers to very short contagion events, with effects limited to the day of the auction. The inter-day approach also includes contagion transmitted from past auctions. In this way,

it is possible to disentangle a pure spatial contagion (intra-day) from a mixed spatial and temporal contagion (inter-day).

Therefore, the output of the models can help to provide answers, both theoretically and empirically, as to how zone interconnections, structural and regulatory changes, congestion, and the quantity of renewable sources affect zonal prices. A clear overview of these interconnections would provide a platform to deduce and design policy. The approach adopted in this paper enables us to identify dominant zones in the spread of systemic risk. In addition, it detects various hidden network structures and relationships between the various zones. The final contribution of this paper is the use of the models with external variables to investigate how short-term interconnectedness relevant for electricity markets are affected by variables connected to prices. A rolling-window procedure for both intra-day and inter-day volatility connectedness over the sample period has been carried out by comparing networks from both models with and without the exogenous variable.

We believe that the findings of the suggested procedure are relevant for policymakers and, if properly taken into account, would ensure good policy design for the proper risk management of energy markets, especially those that are spatial in nature. For instance, they provide a benchmark for the market design mechanism to guide the regulation of network access, facilitate trading in the energy markets and can therefore help to promote efficient network utilization. As highlighted by Bertsch et al. (2017), the design of the European electricity market is based on zonal markets with uniform prices. From a long-term perspective, since the national electricity markets in the European Union have a high potential for improvements via additional capacity investments and the further promotion of market coupling (Gugler et al., 2018), our paper provides a unique data-driven case that can help in policymaking and taking actionable decisions to achieve a well-integrated and efficient European market. The application of the procedure utilized in this paper provides a platform for making optimal environmental and energy policies, especially when the different congestion events and regimes identified are considered for investment decisions.

The remaining sections of the paper are organized as follows: section 2 reviews the literature on risk propagation, interconnections and linkages in energy markets. Section 3 provides an overview of the structure of the Italian zonal market and details the various market operations in the zonal electricity market. Section 4 presents the underpinning of the graphic methodology used in the paper. The data in the empirical section and results are presented and discussed in section 5. Finally, section 6 sets out some concluding remarks and policy recommendations for policymakers, market participants, regulators and governments.

2. Literature review

The theoretical and empirical literature has so far dealt with price differentials from both the supply and demand side, starting with Bigerna and Bollino (2016). As is well known, in the zonal day-ahead market (MGP: Mercato del Giorno Prima) the so-called "market splitting" occurs in the event of congestion. In this case, prices in contiguous market zones are different because, in the market zone where the supply of electricity is lower than the demand, the prices are higher. Due to market congestion, the Ancillary Services Market (ASM) must be activated in order to find a balance between supply and demand (Cappers et al., 2013). Prices on the ASM may differ greatly from prices on the MGP with a significant risk of price hikes for end users (Lamadrid and Mount, 2012; Lisi and Edoli, 2018). Market

congestion is a source of concern for market regulators, who must always ensure the right balance between supply and demand in order to avoid power outages (Weron, 2000).

Another source of risk in electricity markets is price spikes (Grossi and Nan, 2019). Extreme price changes are common in electricity price time series because electricity cannot be economically stored and must be delivered immediately. It is worth noting that risks from spikes can spread from one zone to others creating a contagion effect (Weron, 2014). A further source of contagion, as observed in recent years, is associated with the massive introduction of renewable sources (RES) such as solar and wind energy (Pham, 2019).[1]

The intermittent nature of RES increases the volatility of prices in zones where solar and particularly wind plants are common and this additional volatility can spread to other zones through contagion (Sapio, 2019). Energy market risks affecting market participants, including wholesalers, retailers, and consumers, can be hedged by resorting to futures contracts, but this involves high costs normally reflected in retail prices on deregulated markets (Caldana et al., 2017; Trueck and Weron, 2016).

Consequently, it is essential to study how different types of risk are transmitted from one zone to another. To the best of our knowledge, while many papers have been published dealing with contagion and systemic risk in financial markets, very few empirical studies exist on contagion in energy markets. They include Lautier and Raynaud (2012); Pierret (2013) and, more recently, Bollino et al. (2012), and Bigerna et al. (2017) among others. This paper provides a first-time approach to the use of network analysis in order to examine the direction of contagion in electricity markets. In addition, given the design of the European electricity market, which portrays zonal markets with uniform prices, as mentioned by Bertsch et al. (2017), our methodology is therefore not simply limited to the Italian zonal market but could be extended and utilized in relation to any system with zonal or regional features and some form of interconnectedness between zones or regions.

Complex networks are currently gaining ground in various disciplines, for example, in economics, finance, mathematics and so on (see, for example, Acemoglu et al., 2015; Ahelegbey, 2016; Ahelegbey et al., 2016a,b; Ahelegbey and Giudici, 2014; Billio et al., 2012; Diebold and Yilmaz, 2014). The use of complex networks has helped to extract hidden information from various complex systems. In terms of the energy market, it pinpoints the centrality of networks and the volatility that spreads over other networks. It helps market participants such as traders, investors and regulators to guard against sudden systemic failures which can negatively impact on many businesses and economies because of the significant socio-economic impact of energy in the global economy.

Unlike any other, this paper develops and applies Bayesian Graphical Vector AutoRegression with external regressors (BG-VARX), based on the recent Bayesian Graphical Vector AutoRegression model put forward by Ahelegbey et al. (2016a) in addition to the Bayesian Graphical Structural Equation model (BG-SEMX), thereby incorporating exogenous (i.e. BG-SEMX) and non-exogenous variables (i.e. BG-SEMX) to investigate the complex network dynamics of zonal electricity markets. The Vector AutoRegressive (VAR) model has been widely

[1]For instance, photovoltaic plants have led to increases in the cost of energy in the evening because of the need for operators of conventional power plants to recover investments and idling costs in a shorter time span, when PV generation is unavailable. The Energy and Gas Regulatory Authority or the "Autorità per l'Energia Elettrica e il Gas (AEEG)" reported to the Senate Industry Commission on 18 April 2012. The share of renewable sources has been increasing over the years due to public policy, which enshrine the 20/20/20 targets of the EU climate and energy package providing incentives in the form of a feed–in premium for solar plants and green certificates for all other renewable energy sources. For a detailed overview, see Schwartz (2012).

applied in econometrics to model temporal dependence and interdependence in systemic risk analysis (Ahelegbey et al., 2016a; Billio et al., 2012; Diebold and Yilmaz, 2014). The Bayesian Graphical VAR (BG-VAR), proposed by Ahelegbey et al. (2016a), presents a framework to model directional relationships in a multivariate time series that can be operationalized as VAR models. The approach is based on a Bayesian procedure and a graphic representation of VAR models. The methodology involves inferring the underlying dependence structure of the model in which the coefficients of the relevant covariates have to be selected and estimated. This setting naturally produces sparse and parsimonious models for effective forecasts and easy interpretation. Knowledge of the underlying dependence structures can help researchers and policymakers to understand directional or causal relationships among market variables. Furthermore, such structures can be visualized to provide insight into the connectivity pattern between variables and to identify communities and channels for risk propagation. For regulators, this captures and helps to identify the central zones that can cause a systemic breakdown when severely affected, and to advance policy measures to ensure the stability of the electricity market.

As pointed out by Creti and Fontini (2019), the main challenge of network regulators in various developed countries is how to synchronize regulatory frameworks in the context of the penetration of renewable energy sources allowing them to pursue such traditional aims as adequacy, efficiency and security of infrastructures, while serving customers and remaining customer-friendly. Nonetheless, energy markets continue to undergo regulatory change and a recent paper by Ciferri et al. (2020) investigates the degree of integration using wholesale electricity prices for countries such as Italy, France, the Netherlands, Poland, and the integrated market of Germany and Austria. Ciferri et al. (2020) highlight the fact that that exogenous shocks have permanent effects and orthogonalized shocks largely affect the variance of neighboring markets.

3. The Italian zonal electricity market

There are several reasons to study the risk spreading mechanism in the Italian electricity market. First, the geographical structure of the Italian zonal market naturally shows how risk is transmitted to/received by different zones connected by transmission cables which are prone to congestion. Moreover, the Italian market has seen an increase in renewable sources in the generation mix. The intermittent nature of renewables, particularly wind, increases the exposure of the electricity system to the risk of supply shortages (Wozabal et al., 2016). Considering that the future integrated European market will have a structure similar to that of a zonal market and given the sharp increase in renewable sources in the most important European national markets, the Italian market can show how risk could spread between the areas of the future integrated European market. Another point that makes the Italian market an interesting case is its extreme transparency in terms of available data. Full data on single bids and offers made by market operators are made freely available on the website of the Italian electricity market management company (GME, Gestore del Mercato Elettrico). As such, in recent years, the Italian market has become one of the most intensely analyzed in terms of price forecasting, measuring market power and, very recently, risk assessment (Graf et al., 2020).

This section provides an overview of the Italian zonal power market. The Italian electricity market is called the Italian power exchange (IPEX) and comprises a spot market, a forward market and an over-the-counter (OTC) session, which provides a platform for the

physical delivery of contracts. The spot market comprises three types of markets: the day-ahead (MGP), the intra-day (MI: Mercati Infra-giornalieri) with 7 sessions, and the ancillary services markets (MSD: Mercato dei Servizi di Dispacciamento).[2] GME (Gestore dei Mercati Elettrici) manages the IPEX together with the OTC registration platform for forward electricity contracts stipulated on the bidding system. The market embeds 7 foreign virtual zones, 6 physical zones (see Figure 1 and Table 1, Panel 1) and 5 poles of limited production (national virtual zones)[3]. The physical zones analyzed in this paper are the North (NORD), Center-North (CNOR), Center-South (CSUD), South (SUD), Sardinia (SARD) and Sicily (SIC) (see Figure 1).

A physical zone is a portion of the power grid, with - for system security purposes - physical limits to the transfer of electricity to/from other geographical zones. Figure 2 gives further details of the structure of the Italian zonal market in the current regulatory framework. Zonal prices are the market clearing prices, which are characteristic of each physical and virtual zone in the Day–Ahead Market[4]. The equilibrium price is determined hourly by the intersection of supply and demand curves, see Fianu (2015) for further details. Constraints in inter-zonal capacity often lead to congestion in the grid. Congestion involves different market clearing prices in two zones, creating potential market imperfections. In terms of the operational paradigm, the market is divided into two macro-zones, North and South, with generators located in both. The role of the Market Operator (MO) is to coordinate consumption and generation via the day-ahead market, which is organized on an hourly basis. Therefore, at the beginning of every hour, the MO invites generators to submit a menu of prices at which they are willing to supply with corresponding quantities. The MO, then, forecasts market demands in the various zones. Given the location of each generator and the demand in various zones, the MO solves the optimal dispatch problem subject to an exogenous set of inter-zonal transmission constraints[5]. This determines optimal prices every hour in every zone, along with the quantity of transfer between the zones (see Boffa et al., 2010).

In the event of congestion, and following demonstrations by Bigerna and Bollino (2016), the IPEX is segmented into a variable number of market zones (NoZ), ($1 \leq NoZ \leq 6$); we denote this configuration as the "NoZ-market". It is worth noting that each of these configurations consists of NoZ "markets" that possesses different characterizations of the system marginal price (SMP), called PnZ. Each physical zone belongs to a particular market configuration (see Table 1, Panel 2). For example, if NoZ is equal to two, this means there are several two-market configurations; if three, there several three-market configurations. A two-market configuration can be ML:SARD and SIC, ML:SIC and SARD, ITA:eNORD and NORD, etc., as shown in Table 1, Panel 2. In the case of the two-market configuration "ML:SARD and SIC", the physical zone SIC is a market zone on its own with a PnZ, while ML:SARD is a market zone made up of the interconnections between the physical zones of NORD, CNOR, CSUD, SUD and SARD. In a three-market configuration, for instance, we could have the following market zones: ML, SIC and SARD. Given the time span under consideration, we account for a total of 52,588 hours. Many different market configurations were observed throughout the period (Table 2). For instance, one-market (ITA) occurred for

[2]Abbreviations are of Italian market names. See http://www.mercatoelettrico.org/en/Mercati/MercatoElettrico/MPE.aspx.

[3]https://www.terna.it/en-gb/sistemaelettrico/mercatoelettrico.aspx

[4]The Day–Ahead Market hosts most of the electricity transactions.

[5]The aim of optimal dispatch is to minimize the total electricity expenditure of consumers.

12,389 hours (23.56% of the total period). Four- and five-market configurations accounted for 2.81% (equivalent to 1,467 hours) of the total number of hours. Two- and three-market configurations are the most common, totalling 38,718 hours, accounting for 73.63% of the total number.[6]

Table 2 also shows annual equilibrium price statistics for various market configurations from one-market to five-market zones. Focusing on the most frequent configurations (one to three-market configurations), as the table shows, the higher the complexity of the configuration the higher the average price and corresponding volatility, measured by the standard deviation. This is expected, as the splitting of the market is due to congestion events which usually cause higher prices and volatility in some market zones. Prices decrease in 2016 and then increase until 2018; there is a downward trend in 2019 compared to the previous year. The equilibrium prices that result in the most frequent configurations (one-, two-and three-market configurations) contribute to about 97.20% of the hours in the whole period as shown in Table 2. Table 3 gives summary statistics related to the main market zones illustrated Table 1.The main market zones have a price range from 0.00 to 276.00 Euro/MWh with obvious price variations between the different configurations. The overall average price in the one-market configuration is 48.8 Euro/MWh. The price differential in the two-market configuration, specifically, ML:SARD and SIC lies within the range of 51.17 versus 63.17 Euro/MWh compared to that of ML:SIC against SARD corresponding to 53.51 and 51.46 Euro/MWh, respectively.

Physical Zones	Acronym	
North Italy	NORD	
Center-North Italy	CNOR	
Center-South Italy	CSUD	
South Italy	SUD	
Sardinia	SARD	
Sicily	SIC	
Main market zones	**Components (Physical zones)**	**Acronym**
Italy	NORD:CNOR:SARD:CSUD:SUD:SIC	ITA
Mainland	NORD:CNOR:CSUD:SUD	ML
Mainland and Sicily	NORD:CNOR:CSUD:SUD:SIC	ML:SIC
Mainland and Sardinia	NORD:CNOR:SARD:CSUD:SUD	ML:SARD
Italy excluding North Italy	CNOR:SARD:CSUD:SUD:SIC	ITA:eNORD
Italy excluding North Italy and Sicily	CNOR:SARD:CSUD:SUD	ITA:eNORD:eSIC
Italy excluding North Italy and Sardinia	CNOR:CSUD:SUD:SIC	ITA:eNORD:eSARD

Table 1: Main market zones in the IPEX electricity market.

In a framework similar to the one studied by Gianfreda and Grossi (2012) concerning congestion analysis, congestion can be assumed to occur every time we observe different zonal prices between couples of contiguous zones. Table 4 shows the frequency of congestion between each of the physical zones in Mainland Italy and the other connected physical zones. For example, the second row shows frequencies when prices in CNOR differ from those in NORD, CSUD and SARD and thus provide an indication of congestion between selected configurations. Comparatively, over various years and with various configurations, the highest

[6]The six-market configuration was observed over just 4 hours, so the corresponding statistics have been omitted from the table.

	Year	2014	2015	2016	2017	2018	2019	2014-2019
One Mkt	Mean	47.30	47.69	41.88	47.75	55.25	47.24	48.80
	Std. Dev.	16.07	13.22	12.83	15.18	13.34	11.74	14.16
	Frequencies	716	978	1,740	2,577	3,354	3,024	12,389
	%	**1.36%**	**1.86%**	**3.31%**	**4.90%**	**6.38%**	**5.75%**	**23.56%**
Two Mkts	Mean	54.82	52.36	42.53	55.01	65.29	56.16	53.99
	Std. Dev.	23.76	13.91	13.60	16.60	17.72	18.22	18.84
	Frequencies	5,147	5,222	4,769	4,318	4,028	4,176	27,660
	%	**9.79%**	**9.93%**	**9.07%**	**8.21%**	**7.66%**	**7.94%**	**52.60%**
Three Mkts	Mean	57.42	53.94	44.03	58.90	70.15	59.05	56.10
	Std. Dev.	28.45	15.63	14.09	20.25	20.33	19.82	21.96
	Frequencies	2,595	2,161	2,022	1,676	1,195	1,409	11,058
	%	**4.93%**	**4.11%**	**3.84%**	**3.19%**	**2.27%**	**2.68%**	**21.03%**
Four Mkts	Mean	52.04	51.13	42.19	57.89	62.04	55.60	52.48
	Std. Dev.	28.97	14.44	14.68	23.23	19.51	18.22	21.26
	Frequencies	299	378	240	174	178	151	1,420
	%	**0.57%**	**0.72%**	**0.46%**	**0.33%**	**0.34%**	**0.29%**	**2.70%**
Five Mkts	Mean	56.70	47.55	42.52	62.76	65.97	-	52.04
	Std. Dev.	33.81	15.13	16.96	23.50	16.42	-	20.61
	Frequencies	2	22	14	13	6	0	57
	%	**0.00%**	**0.04%**	**0.03%**	**0.02%**	**0.01%**	**0.00%**	**0.11%**

Table 2: IPEX market configurations (2014-2019). Descriptive statistics of prices and number of hours (frequencies) for the different configurations. Percentages in terms of total hours in the period 2014-2019.

Market configurations (No. of hours)	Market zones (with components)	Mean	SD	Min.	Max.
One-market (12389)					
ITA	NORD:CNOR:CSUD:SUD: SIC:SARD	48.80	14.16	1.00	170.00
Two-market (25036)					
ML:SARD-SIC (20972)	NORD:CNOR:CSUD:SUD:SARD	51.17	15.14	0.84	170.00
	SIC	63.17	26.84	0.00	259.03
ML:SIC-SARD (205)	NORD:CNOR:CSUD:SUD:SIC	53.51	15.68	1.00	170.00
	SARD	51.46	16.92	0.00	276.16
ITA:eNORD-NORD (2116)	CNOR:CSUD:SUD:SIC:SARD	53.40	15.96	0.00	170.99
	NORD	52.01	16.16	1.00	206.12
Three-market (13537)		51.09			
ML-SA-SI (824)	NORD:CNOR:CSUD:SUD	51.09	15.07	1.00	170.00
	SARD	51.46	16.92	0.00	276.16
	SIC	63.17	26.84	0.00	259.03
ITA:eNORD:eSIC (3958)	NORD	52.01	16.16	1.00	206.12
	CNOR:CSUD:SUD:SARD	50.96	15.30	0.00	170.99
	SIC	63.17	26.84	0.00	259.03

Table 3: Summary statistics of prices in main market zones.

frequency of congestion (15.19%) was between NORD and CNOR in 2018. On the other hand, the configuration CSUD connected with SARD, SUD and CNOR suffered no congestion in 2014 and 2016.

In recent years, the Italian energy market has undergone various regulatory transformations, which have helped to ensure fair competition among market participants. Indeed, the development of electricity networks and the excess of supply due to the reduction in demand

	2014	2015	2016	2017	2018	2019
NORD vs CNOR	13.88%	13.37%	12.46%	14.82%	15.19%	14.88%
CNOR vs NORD-CSUD-SARD	0.13%	0.17%	0.53%	0.47%	0.41%	0.39%
CSUD vs SARD-SUD-CNOR	0.00%	0.01%	0.00%	0.03%	0.02%	0.01%
SUD vs CSUD-SIC	1.56%	2.24%	2.02%	1.98%	1.26%	0.73%

Table 4: Frequencies of congestion events according to various zone configurations in alignment with physical grid interconnections (2014-2019)

and growth in renewable energy sources have enhanced competition in electricity markets in Italy. Legislative Decree 28/11 came into effect in 2012, transforming incentives for renewable sources.[7]

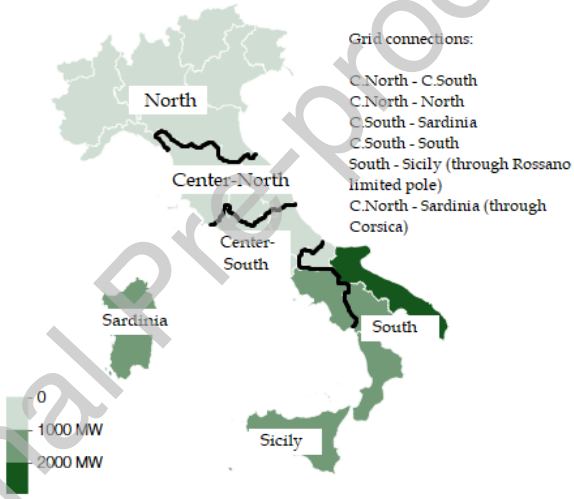

Figure 1: Map of Italy with the regional distribution of installed wind energy capacity (in varying degrees of green) in 2016 and the borders between zones in the transmission grid (thick black lines). The zonal connections, in the top right corner, show the basic structure of the market—physical zones. Source: processing by the authors.

In 2016, the Italian government passed a decree supporting incentives for renewable energy sources in addition to photovoltaic systems. The introduction of market coupling with Slovenia, Austria and France provides significant benefits by reducing inefficiencies in the allocation of rights for cross-border transmission capacity. The internal grid was modified and upgraded in 2012, allowing for improved integration between market zones and consequently the improved transmission of electricity throughout CSUD and SUD zones.

[7]For instance, the green certificate mechanism was replaced by feed-in tariffs, with maximum allowable expenditure to provide incentives for capacity with auction procedures reserved for large plants. However, in 2013, a new national energy strategy was approved and confirmed by the Italian government. In the wholesale market, competition is growing continually. For example, the market share of the four largest operators decreased by 5% in 2012 compared to 2011 (49%). Specifically, ENEL remains the main market operator with 25% of the market (26% in 2011), followed by ENI (9%), Edison (7.2%) and E.On (4.4%). Correspondingly, the collective shares of small operators increased to 30.2%.

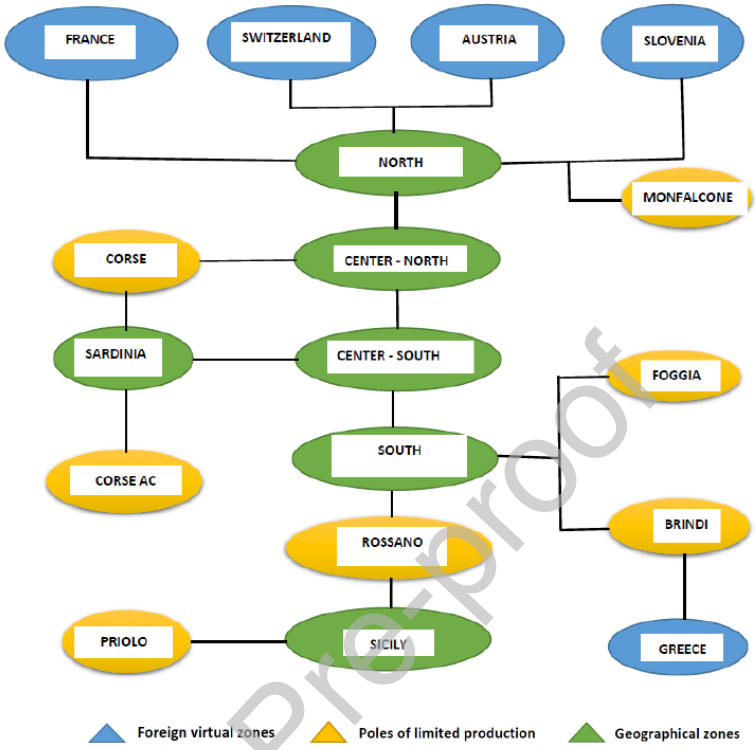

Figure 2: The structure of the Italian zonal market. *Source*: Processing by the authors based on a map by Terna

.

4. Model Formulation and Estimation

We model the zonal risk channels by decoupling the path of influence as: 1) intra-day (within-day) effects; and 2) inter-day (between-day) spillovers. The intra-day captures spillover channels that occur within the same day, while the inter-day measures spillovers between zones with a time-lag. We model the intra-day and inter-day dependencies from multivariate time series using, respectively, a simultaneous equation and a vector autoregressive model with exogenous factors.

4.1. Modeling Intra-day Dependence

Let $Y_t = (Y_{1,t}, \ldots, Y_{n,t})$ be the vector of log price volatilities in n zones at time t. We model the intra-day pattern of dependence among zones via a panel structural equation model with exogenous factors (SEMX) with the i-th equation given by:

$$Y_{i,t} = \sum_{i \neq j=1}^{n} B_{ij|y} Y_{j,t} + B_{i|d} D_{i,t} + B_{i|f} F_{i,t} + B_{i|w} W_{i,t} + U_{i,t} \tag{1}$$

where $D_{i,t}$, $F_{i,t}$ and $W_{i,t}$ are the log transformation of daily electricity demand, forecast electricity demand and forecast wind generation, respectively, for zone i, $B_{i|d}$, $B_{i|f}$ and $B_{i|w}$

capturing the effect of these exogenous macro factors on $Y_{i,t}$. $B_{ij|y}$ measures the effect of Y_j on Y_i at time t, and U_t is a vector of error terms assumed to be independent and identically distributed, $U_t \sim \mathcal{N}(0, \Sigma_u)$. We define $B_{\cdot|y}$ as a full (non-symmetric) matrix with zeroes on the main diagonal that records the contemporaneous effects among $Y_{i,t}$. The matrix form of (1) is given by

$$Y_t = BX_t + U_t = B_{y|y}Y_t + B_{y|z}Z_t + U_t, \qquad U_t \sim \mathcal{N}(0, \Sigma_u) \tag{2}$$

where $B = (B_{y|y}, B_{y|z})$, $X_t = (Y_t', Z_t')'$, $Z_t = (D_{1,t}, \ldots, D_{n,t}, F_{1,t}, \ldots, F_{n,t}, W_{1,t}, \ldots, W_{n,t})$ is a collection of the zonal specific exogenous macro factors (in our case actual/forecast electricity demand and wind generation). $B_{y|z} = (B_{y|d}, B_{y|f}, B_{y|w})$ is a stacked collection of coefficient matrices $B_{y|d}$, $B_{y|f}$ and $B_{y|w}$ each of dimension $n \times n$ with zero off-diagonal elements and only the main diagonals contain coefficients of the effects of the exogenous factors for each zone. Our focus here is to analyze the direction of influence between zones as shown in Figure 3.

$$B_{y|y} = \begin{pmatrix} 0 & 0 & 0 & 0 & 0 \\ \beta_{21} & 0 & 0 & 0 & 0 \\ \beta_{31} & 0 & 0 & 0 & 0 \\ 0 & \beta_{42} & 0 & 0 & \beta_{45} \\ \beta_{51} & 0 & \beta_{53} & 0 & 0 \end{pmatrix} \Longrightarrow$$

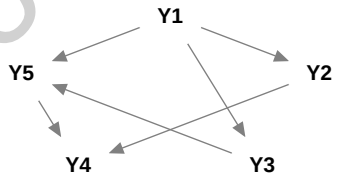

Figure 3: Coefficient matrix and the associated network structure. The non-zero elements in $B_{y|y}$ are real numbers. The column and row labels of $B_{y|y}$ are $(Y_1, Y_2, Y_3, Y_4, Y_5)$ at time t. Links in the network are related to the non-zero elements in $B_{y|y}$ and are directed from column labels to row labels.

4.2. Modeling Inter-day Dependence

We model the inter-day dependence via a panel VAR (or VARX) model of n units

$$Y_t = BX_t + V_t = \sum_{l=1}^{p} A_{l,y|y}Y_{t-l} + A_{y|z}Z_t + V_t, \qquad V_t \sim \mathcal{N}(0, \Sigma_v) \tag{3}$$

where p is the lag order; $B = (A_{1,y|y}, \ldots, A_{p,y|y}, A_{y|z})$, $X_t = (Y_{t-1}', \ldots, Y_{t-p}', Z_t')'$, $A_{l,y|y}$ is the coefficients matrix at lag l; $A_{y|z}$ is a zero off-diagonal coefficients matrix; Z_t is a set of zonal-specific macro variables; $A_{y|z} = (A_{y|d}, A_{y|f}, A_{y|w})$ is a stacked representation of coefficient matrices $A_{y|d}$, $A_{y|f}$ and $A_{y|w}$ each of dimension, $n \times n$ with zero off-diagonal elements and only the main diagonals contain coefficients of the effects of the exogenous factors for each zone.

The difference between the model presented in (3) and that of Ahelegbey et al. (2016a) is that the exogenous variables Z_t of the current model are equation-specific factors instead of common factors. Thus, the current version is a panel structure model instead of standard VAR model with exogenous factors.

Inter-day networks generally comprise own-lagged and cross-lagged dependencies. In this application, we follow a concept similar to that of Granger causality (Granger, 1969) by focusing on the cross-lagged dependencies. See Figure 4 for an illustration.

4.3. Bayesian Graphical Network Model Estimation

The application of the Bayesian graph-based approach in the current work is to model separately the intra-day and inter-day volatility spillover among zones of an electricity market

$$A_{1,y|y} = \begin{pmatrix} \alpha_{11} & 0 & 0 & 0 & 0 \\ \alpha_{21} & 0 & \alpha_{23} & 0 & 0 \\ \alpha_{31} & 0 & \alpha_{33} & \alpha_{34} & 0 \\ 0 & 0 & \alpha_{43} & \alpha_{44} & 0 \\ 0 & \alpha_{52} & 0 & 0 & \alpha_{55} \end{pmatrix} \implies$$

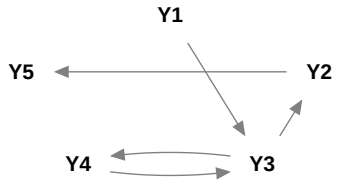

Figure 4: Coefficient matrix of a VAR(1) model and the associated cross-lagged network. The column labels of $A_{y|y}$ are lags of $(Y_1, Y_2, Y_3, Y_4, Y_5)$ and row labels are at time t. Links in the network are results of non-zero elements in $A_{y|y}$ and are directed from column labels to row labels.

via a panel structure of the data for purposes of interpretability and to produce a parsimonious specification of the model.

The introduction of networks in a typical multivariate regression model helps to interpret the relationships in the model. To formalize this representation, equations (2) and (3) can be specified through the lens of networks by assigning to each coefficient B_{ij} a latent variable inclusion indicator, $G_{ij} \in \{0, 1\}$, such that for $i, j = 1, \ldots, n$:

$$B_{ij} = \begin{cases} 0 & \text{if } G_{ij} = 0 \implies Y_j \not\to Y_i \\ b_{ij} \in \mathbb{R} & \text{if } G_{ij} = 1 \implies Y_j \to Y_i \end{cases} \tag{4}$$

where $Y_j \not\to Y_i$ means that Y_j does not influence Y_i. Thus, the objective of the network model is to learn the sparse latent dependence structure, G, and the associated coefficients matrix, B, which measures the weights and signs of the dependence structure in the data.

Estimating jointly the parameters of the BG-SEMX in (2), or the BG-VARX in (3), or the simplified regression model is a challenging problem and a computationally intensive exercise. We specify the prior distributions as follows:

$$[B_{ij}|G_{ij} = 1] \sim \mathcal{N}(0, \eta), \qquad G_{ij} \sim \mathcal{B}er(\pi_{ij}), \qquad \Sigma_\varepsilon \sim \mathcal{W}(\delta, \Lambda_0)$$

where η, π_{ij}, δ, and Λ_0 are hyper-parameters. The specification for B_{ij} conditioned on G_{ij} follows a normal distribution with zero mean and variance η. Therefore, the relevant explanatory variables with significant information to predict a response variable are associated with coefficients different from zero and the rest (representing variables that are not relevant) are restricted to zero. We consider G_{ij} as Bernoulli distributed with π_{ij} as the prior probability. Finally, we assume Σ_ε^{-1} is Wishart distributed with prior expectation $\frac{1}{\delta}\Lambda_0$ and $\delta > n$ as the degrees of freedom parameter.

Let Y_t be the vector of log volatilities of the zones and X_t the vector of explanatory variables at time t. In addition, let $Y = (Y_1, \ldots, Y_T)$ and $X = (X_1, \ldots, X_T)$ denote a collection of Y_t and X_t over a fixed window of length T. Following the Bayesian framework of Geiger and Heckerman (2002), the structural parameters can be integrated out analytically to obtain a marginal likelihood function over the graphs. This allows for the application of an efficient Gibbs sampling algorithm to sample the graph structure and the model parameters in blocks. In order to approximate the graph and parameters posterior distribution, we consider a collapsed Gibbs sampler that proceeds as follows:

1. sample via a Metropolis-within-Gibbs $[G|Y, X]$ (see Algorithms 1 and 2 in Appendix A);
2. sample from $[B, \Sigma_\varepsilon|Y, X]$ by iterating the following steps:

(a) sample $[B_{i,\pi_i}|Y, X, \hat{G}, \Sigma_\varepsilon] \sim \mathcal{N}(\hat{B}_{i,\pi_i},\ Q_{\pi_i})$ where

$$\hat{B}_{i,\pi_i} = \sigma_{\varepsilon,i}^{-2} Q_{\pi_i} X'_{\pi_i} Y_i, \qquad Q_{\pi_i} = (\eta^{-1} I_{d_x} + \sigma_{\varepsilon,i}^{-2} X'_{\pi_i} X_{\pi_i})^{-1} \tag{5}$$

where $X_{\pi_i} \in X$ is the set of predictors of Y_i that corresponds to $(\hat{G}_{y_i,x_\pi} = 1)$, $\sigma^2_{\varepsilon,i}$ is the i-th diagonal element of $\hat{\Sigma}_\varepsilon$, and d_x is the number of covariates in X_{π_i}.

(b) sample $[\Sigma_\varepsilon^{-1}|Y, X, \hat{G}, B] \sim \mathcal{W}(\delta + N,\ \Lambda_T)$ where

$$\Lambda_T = \Lambda_0 + (Y - X\hat{B}')'(Y - X\hat{B}') \tag{6}$$

For further details concerning the network sampling algorithm and convergence diagnostics, refer to Appendix A for an overview.

4.3.1. Lasso Regularization Method

We apply the Lasso regularization by Tibshirani (1996) as a benchmark model for our empirical analysis. This approach estimates the coefficients of a regression model by solving:

$$\hat{B}_{ij} = \min_{B_{ij}} \left\{ \sum_{t=1}^{T} \left(Y_{i,t} - \sum_{j=1}^{q} B_{ij} X_{j,t} \right)^2 + \lambda \sum_{j=1}^{q} |B_{ij}| \right\} \tag{7}$$

where T is the number of observations, q is the number of covariates, λ is the penalty term such that high values shrinks a large number of the coefficients towards zero. In the empirical exercise, we select the regularization parameter, $\lambda \cdot 1se$, that corresponds to one standard error from the minimum mean square cross-validated errors.

5. Modeling risk contagion and applications

Network analysis is currently gaining ground in various disciplines given the fact that almost everything seems to have some kind of interrelationship. Network analysis and its applications, especially in energy markets is no different. With the energy revolution taking place in various countries, the slow but steady transition from non-renewable energy sources is faced by investors and regulators with different forms of uncertainty. The Italian electricity market, with its zonal structure and the close interconnections between zones, provides an ideal framework for original network analysis.

We analyze intra-day and inter-day volatility spill-over channels among the physical zones of the Italian market, characterizing the dynamics of the networks via a yearly (365-day) rolling window. We set the increments between consecutive rolling windows at a one-month.

The first rolling window is from March 2014 - February 2015, followed by April 2014 - March 2015, and the last from January 2019 - December 2019. In all, there are 59 rolling windows. The primary objective of our empirical exercise is to investigate the joint impact of the exogenous macro causes of volatility (in our case actual/forecast electricity demand and forecast wind generation) on volatility spill-over in the Italian zonal electricity market. Section 5.2 and 5.3 present our findings for the above research goal, respectively, for the intra-day and inter-day volatility channels of contagion.

5.1. Data description

Hourly spot prices (in the day-ahead market) in the 6 physical zones of the Italian electricity market from January 2014 to December 2019 are obtained from the Italian Electricity Market Management website. We also utilize actual/forecast electricity demand and forecast wind generation in the Italian zonal electricity market between March 2014 and December 2019.[8] We analyze the physical zones of the North (NORD), Central-North (CNOR), Central-South (CSUD), South (SUD), Sardinia (SARD) and Sicily (SIC).

Suppose that $P_{i,l,t}$ is the observed price for the i-th zone at the l-th hour of day t. We construct daily standard deviations ($\sigma_{i,t}$) as a measure of realized volatility by:

$$\sigma_{i,t} = \sqrt{\frac{1}{N-1}\sum_{l=1}^{N}(P_{i,l,t} - \bar{P}_{i,t})^2} \tag{8}$$

where $\bar{P}_{i,t}$ is the average of P_i on day t and N is the total number of observations in a day, i.e., $N = 24$. This formula was used to compute standard deviations for prices.[9]

Figure 5 sets out the time dynamics of daily electricity prices and volatility in the Italian zonal power market in the period 2014-2019. They highlight variations in electricity prices in the various zones. A quick glimpse at the prices and volatilities shows some co-movements in the evolution of the time series, which initially confirm the existence of some form of structure in the various zones. The autocorrelation functions of log-volatility are shown in Appendix Appendix B, Figure B.1. The distribution of daily log-volatilities shows non-negative values virtually throughout the sample period. From the various multivariate regression models presented in the previous section, the error terms of the models are assumed to be drawn from a multivariate Gaussian distribution. To satisfy this condition, we standardize the log-volatility series to a zero mean and unit variance.

Table 5 gives the descriptive statistics of the daily log-volatility of prices and log-transformation of the exogenous factors for physical zones in terms of mean, standard deviation, minimum, maximum, skewness, excess kurtosis, and Jaque-Bera test. SIC and SARD (although very close to SIC) recorded the minimum and maximum daily price volatilities, respectively, over the sample period.[10] On average, the price volatility in the NORD zone was lower than the SUD. With the exception of SIC, which appeared to be negatively skewed (-1.3) with higher

[8] Day-ahead prices were downloaded from the website of the Italian Regulator for the electricity market (GME), `www.mercatoelettrico.org`. Forecast electricity generation from wind and actual and forecast electricity demand (one day-ahead horizon) data were obtained from the website of the Italian TSO Terna, `www.terna.it`. Complete data from Terna are available only from the beginning of March 2014.

[9] We are aware that the choice of the daily summary index of volatility is not neutral in relation to the model estimation. In this section, the usage of the unweighted mean and the standard deviation means that all hourly prices have the same weight for the daily outcome. Moreover, the 24 hourly prices used to compute the daily average price and the daily volatility measure may refer to different market zones, because on a given day a physical zone may be isolated for some hours and on others may connect to form a different market zone. This is a source of bias for the analysis. However, we assume that when multiple-market zones are created, prices are less volatile and this should be reflected by low volatility. In order to see the effect of different choices of the daily aggregation on risk contagion, we carried out the same analysis using a robust version of daily volatility given by the Median Absolute Deviation (MAD). The results are shown and discussed in section 5.5. The authors are grateful to one of the referees, who raised this point, and for for the opportunity to highlight the impact the selection of a daily aggregation formula can have on the final results.

[10] High prices and volatility in Sicily were examined by Sapio and Spagnolo (2016) who found evidence of tacit collusion in this zone.

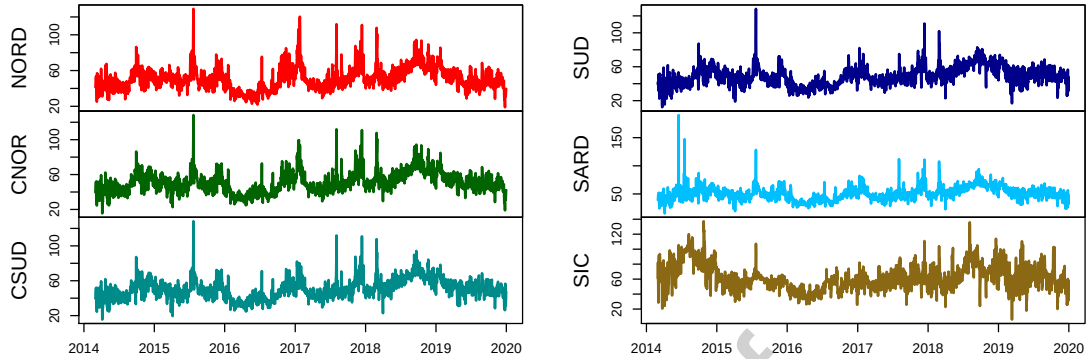

(a) Daily Mean Prices

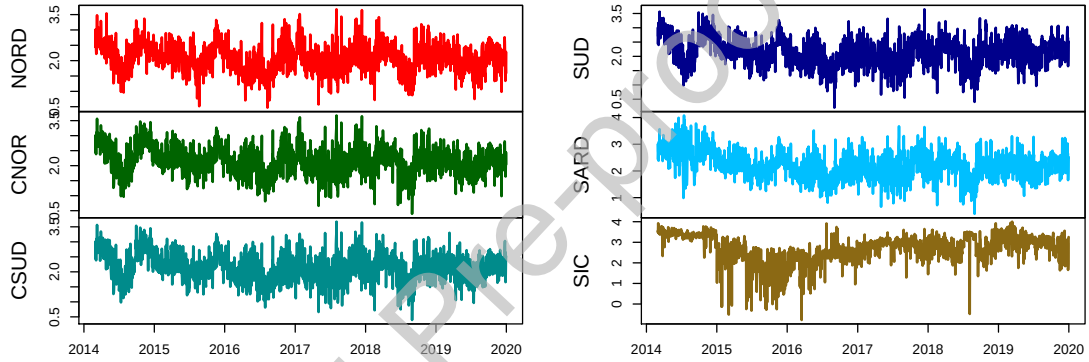

(b) Daily Log-Volatilities

Figure 5: Time series plots of daily mean electricity prices and log daily standard deviations in North (NORD), Central-North (CNOR), Central-South (CSUD), South (SUD), Sardinia (SARD), and Sicily (SIC), between March 1, 2014 and December 31, 2019.

kurtosis (2.875), the remaining zones have an approximately normal distribution with skewness ranging from -0.08 to 0.15, with excess-kurtosis ranging between -0.13 and 0.21. The Jaque-Berra test for normality in the table is represented by the p-values. The test strongly supports normality for NORD, CNOR, CSUD and SUD. However, it rejects normality for SARD and SIC.

We carried out unit root tests (Augmented Dickey–Fuller, ADF, and Phillips–Perron, PP, test) on the time series of log-volatility of zonal prices, which reject the null hypothesis of unit root (see Table 6).

5.2. Intra-day volatility spillover networks

We present the results of the dynamic nature of intra-day zonal log price volatilities interconnectedness over the sample period 2014–2019 and analyze the evolution of four different models: BG-SEMX and Lasso-SEMX, BG-SEM and Lasso-SEM, i.e. two models without exogenous variables and two X inclusive models with exogenous macro factors, i.e., actual/forecast electricity demand and forecast wind generation.[11]

[11] The codes used to estimate the models illustrated in the empirical section have been written in Matlab. An old version of the BG-VAR code is publicly available from Ahelegbey et al. (2016a). The new version of the

	Min	Max	Mean	SD	Skew	Ex.Kurt	JB(*p-value*)
NORD	0.470	3.672	2.091	0.464	0.038	0.147	0.287
CNOR	0.396	3.672	2.159	0.478	0.007	-0.043	0.923
CSUD	0.396	3.672	2.143	0.479	-0.015	-0.109	0.582
SUD	0.206	3.645	2.126	0.493	-0.077	-0.126	0.179
SARD	0.396	4.076	2.204	0.506	0.146	0.206	0.003
SIC	-0.776	4.002	2.721	0.659	-1.300	2.875	0.000
D.NORD	12.430	13.302	12.967	0.179	-0.737	-0.526	0.000
D.CNOR	10.756	11.679	11.289	0.160	-0.523	-0.394	0.000
D.CSUD	11.311	11.994	11.716	0.115	-0.457	-0.007	0.000
D.SUD	10.752	11.549	11.136	0.137	0.183	-0.204	0.000
D.SARD	9.793	10.647	10.129	0.129	1.128	1.481	0.000
D.SIC	10.376	11.045	10.742	0.108	-0.118	-0.048	0.077
FD.NORD	12.403	13.371	12.986	0.191	-0.754	-0.346	0.000
FD.CNOR	10.529	11.779	11.344	0.155	-0.645	-0.071	0.000
FD.CSUD	11.071	12.089	11.728	0.118	-0.347	0.540	0.000
FD.SUD	10.528	11.975	11.131	0.135	0.355	0.892	0.000
FD.SARD	9.455	10.430	10.062	0.094	-0.181	1.977	0.000
FD.SIC	10.446	11.175	10.787	0.107	0.276	0.138	0.000
FW.NORD	0.881	6.579	4.376	0.887	-0.444	-0.230	0.000
FW.CNOR	1.483	7.471	5.669	0.941	-0.619	0.398	0.000
FW.CSUD	0.000	10.425	8.338	1.248	-1.978	8.810	0.000
FW.SUD	6.250	11.384	9.604	0.842	-0.451	-0.238	0.000
FW.SARD	0.000	9.929	7.929	1.159	-1.645	8.134	0.000
FW.SIC	0.000	10.393	8.531	1.083	-2.303	14.712	0.000

Table 5: Descriptive statistics of the daily log-volatilities of prices and log-transformations of exogenous factors in North (NORD), Central-North (CNOR), Central-South (CSUD), South (SUD), Sardinia (SARD) and Sicily (SIC). Note: D.* means actual Demand, FD.* Forecast Demand and FW.* Forecast Wind generation in the * zone.

Test	Type	CNOR	CSUD	NORD	SARD	SIC	SUD	Sig.
ADF	1 lag	-6.60	-6.54	-6.52	-9.64	-8.11	-6.20	***
	1 lag, trend	-19.11	-18.75	-19.60	-19.49	-23.20	-17.00	***
	1 lag, drift	-18.20	-17.69	-18.25	-18.01	-18.65	-16.71	***
PP	1 lag, drift	-833.98	-824.29	-833.98	-765.65	-1103.15	-817.23	***
	1 lag, trend	-24.15	-24.31	-24.32	-23.44	-24.15	-23.45	***

Table 6: Unit root tests on daily log-volatility of prices. Note: *** is 1% level of significance.

With numerical summaries, we characterize the time-varying nature of interconnections by monitoring network density. The density of an n-nodes network is given by:

$$\text{Network Density} = \frac{Total\ Edges\ in\ Estimated\ Network}{Total\ Number\ of\ Possible\ Links}$$

code is available from the authors, upon request. The average time to run 20,000 simulations for the network sampling and model estimation can be summarized as follows:

	SEM	SEMX	VAR	VARX
BG	9.63	12.07	2.67	2.8
Lasso	2.15	3.38	3.89	6.06

The longest time required in the case of BG-SEM are due to the constrains imposed in the acyclic graphs.

For directed graphs, such as the Lasso-SEM networks, the number of possible links is $n(n-1)$, while for Directed-Acyclic-Graphs (DAGs), such as the BG-SEM networks, the number of possible links is $\frac{1}{2}n(n-1)$. This is because, by construction, the Lasso-SEM estimates directed networks that allow bi-directed links. The BG-SEM, on the other hand, infers directed networks without feedbacks (bi-directed links) and cycles. Thus, the DAGs produced by the BG-SEM are naturally suitable for making causal inferences, unlike the Lasso-SEM where it is not possible to distinguish between cause and effects in a directed network.

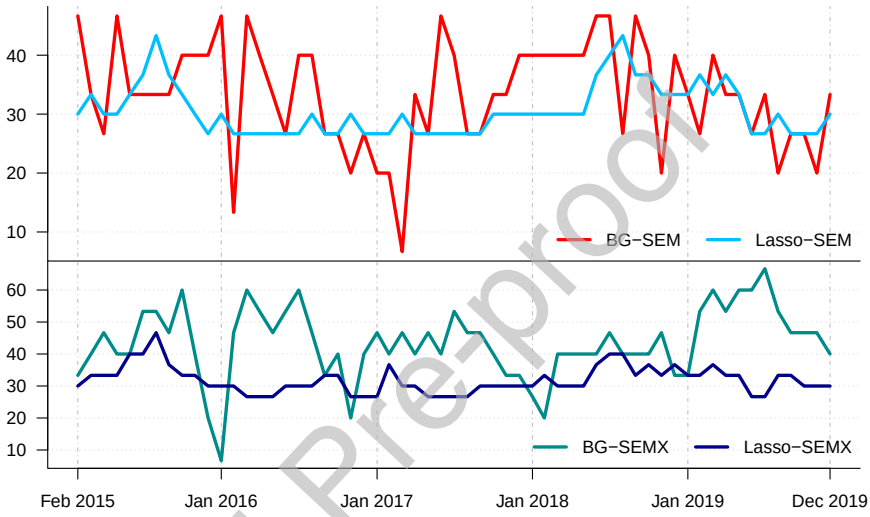

Figure 6: Yearly rolling series of network density from the BG-SEM & SEMX and Lasso-SEM & SEMX.

Figure 6 shows the time series of intra-day volatility network densities for the competing methods from the yearly rolling window estimations over the sample period. The BG-SEM and Lasso-SEM network densities are plotted in the top panel, while the BG-SEMX and Lasso-SEMX are in the bottom panel. The degree of interconnectedness according to the Lasso-SEM and Lasso-SEMX is more stable than that of the BG-SEM and BG-SEMX. The BG-SEM network density exhibits a higher degree of fluctuation than the rest. One takeaway from Figure 6 is that the inclusion of the macro variables (actual/forecast demand and forecast wind generation), have an impact on volatility spillover in the Italian zonal electricity market, since the BG-SEM and BG-SEMX record different network densities.

To assess the impact of the exogenous macro factors on volatility spillover, we compare all four models over two sub-periods: 2015–2017 and 2018–2019.[12]

[12]The year 2015 was very significant in terms of the integration of national electricity markets in the European market and years 2017 and 2018 saw the reversal of the upward trend in fuel prices in the European market. However, the Italian electricity market was affected by French nuclear shutdowns. The average national price (PUN) of the IPEX rose until November 2018 compared to the first eleven months of 2017, due to the increase in fuel prices and CO2 emissions rights. More than all other production methods and technologies, the production of renewable technologies increased by 13.4% up to November 2018. In the same period, wind generation increased by 1.1% and solar energy decreased by 9.3% compared to the same period in 2017. In the year 2019, prices dropped with the PUN falling to levels close to 52 Euros/MWh, due to a continuing trend in line with the fall in gas costs and with European prices. As a result, a "structural" spread of about 12 Euro/Mwh persists. Interestingly, a similar trend can be found in the zones of Italy where price differentials

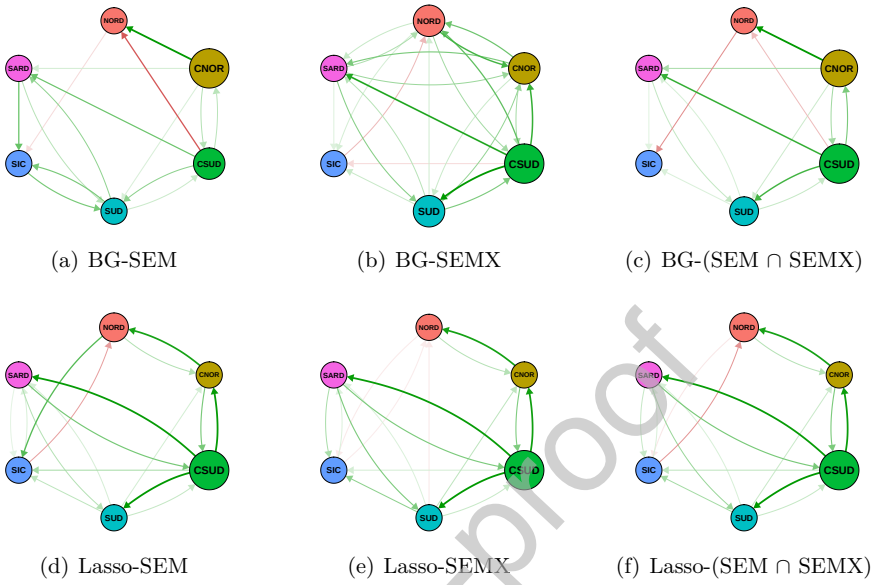

(a) BG-SEM (b) BG-SEMX (c) BG-(SEM ∩ SEMX)

(d) Lasso-SEM (e) Lasso-SEMX (f) Lasso-(SEM ∩ SEMX)

Figure 7: **Averaged Intra-day Networks 2015–2017**. Dark (light) green-links indicate strong (mild) positive impacts, and dark (light) red-links indicate strong (mild) negative effects. The node size is based on hub scores.

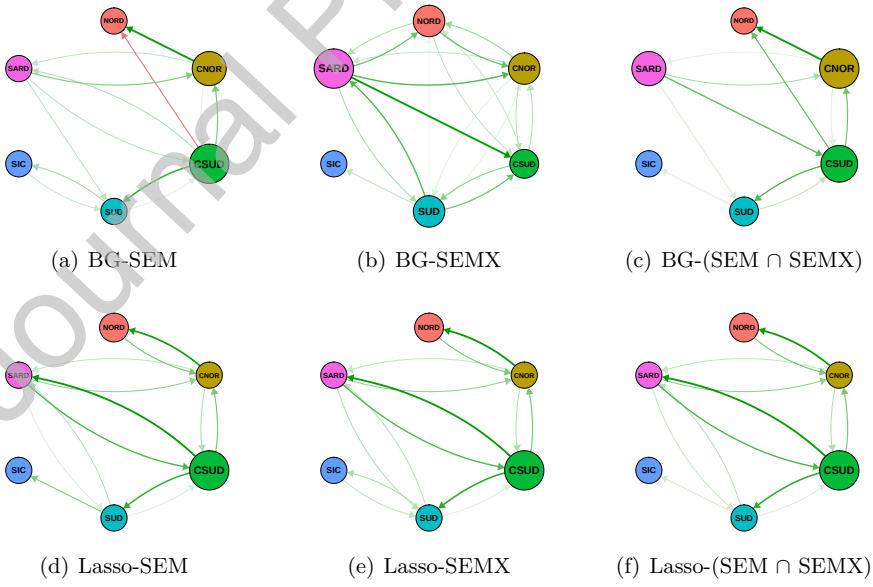

(a) BG-SEM (b) BG-SEMX (c) BG-(SEM ∩ SEMX)

(d) Lasso-SEM (e) Lasso-SEMX (f) Lasso-(SEM ∩ SEMX)

Figure 8: **Averaged Intra-day Networks 2018–2019**. Dark (light) green-links indicate strong (mild) positive impacts, and dark (light) red-links indicate strong (mild) negative effects. The node size is based on hub scores.

between NORD-SUD were nullified along with drops in prices to 0 Euros/Mwh in SIC. Volatility in the market increased in SARD, SUD and SIC, zones characterized by a high share of renewables, albeit in constant supply.

Figures 7 and 8 present the intra-day network topology averaged over the two sub-periods. Figures 7(c) and 7(f) (Figures 8(c) and 8(f)) display network links common to BG-SEM and BG-SEMX (Lasso-SEM and Lasso-SEMX). For cases with a common link that changes sign depending on exogenous variables, we show the common link with the sign of the average coefficients. For the sake of clarity, we used various colors and sizes of nodes and links to depict the network interactions. The size of the nodes is deduced based on weighted out-degrees, i.e. the average of the absolute value of the coefficients weighted by the hub scores. As such, a larger node means that these particular nodes have a stronger impact on the network. A dark green link indicates a strong simultaneous effect, while a light green link signals mild impact. For instance, the BG-SEM network in Figure 7(a) shows that between 2015–2017, the volatility of NORD is strongly positively sensitive to the risk from CNOR, and strongly negatively sensitive to that of CSUD. Furthermore, a light green link from SARD to SUD and a reverse link from SUD to SARD suggest a mild positive impact and are evidence of simultaneity between the two zones. Since the BG-SEM networks are DAGs depicting lead-lag relationships in a simultaneous network, the simultaneity between SARD and SUD indicates that the volatility of one zone may precede the other in some periods, and this relationship may be reversed at other times. Thus, neither of the two zones play a dominant role in terms of influencing the other. CNOR in Figure 7(a) is larger than the rest, suggesting that, between 2015–2017, CNOR plays a significant role in spillover transmission according to the BG-SEM network. When exogenous factors are included in the model, the BG-SEMX reveals CSUD as the central zone for risk propagation. This is confirmed by the other networks in Figure 7.

It is well known that in turbulent times some assets/markets perform generally badly while others have mild reactions. Assets that react negatively are often desirable and sell at a premium. To hedge energy market risk, it is ideal for an investor to select an asset that correlates negatively with others. The BG-SEMX structure in Figure 7(b) shows that, between 2015–2017, NORD exhibited a mild negative sensitivity to risk from SIC, and SIC reacted in like manner to CSUD. However, this observation was not persistent over time and was not recorded in the 2018–2019 sub-period.

Period	Method	SEM	SEMX	SEM ∩ SEMX
2015 – 2017	BG	15	23	14
	Lasso	17	18	17
2018 – 2019	BG	13	19	11
	Lasso	13	14	13

Table 7: Total number of links in intra-day sub-period networks for the competing methods.

Table 7 tabulates the total number of links in the SEM and SEMX network and the topological structure common to the networks. The table shows that, on average, the inclusion of exogenous macro factors increases intra-day volatility interconnectedness between the zones of the market. On average, 2015-2017 saw more interconnectedness than 2018-2019. The SEMX networks also recorded a higher number of links than the SEM. For instance, Table 7 shows a total of 15 links for BG SEM and 23 for BG-SEMX, 14 of them in both. Thus, the

These episodes explain the peaks and troughs represented in the network density plot and motivate the choice to split the period into two sub-periods 2015–2017 and 2018–2019.

BG-SEMX included almost all the connections in the BG-SEM and more. On the other hand, the Lasso-SEMX identified one more link than the Lasso-SEM. The same is true of 2018-2019 sub-period networks. Thus, overall, the macro determinants of volatility increase volatility spill-over in the electricity market.

We now turn our attention to the following question: "In the event of a shock to a zones or a group of zones, which zone will be most central to intra-day volatility spillover propagation in the Italian zonal electricity market?". In other words, which zone or group of zones, when affected by a major shock, will lead to increasing uncertainty in the Italian electricity market?

Answering this question requires the adoption of network measures of centrality to identify the transmitters and receivers of intra-day volatility spill-over in the two sub-periods. Hence, we rank the importance of nodes in the network using hub and authority scores.[13] From a financial viewpoint, nodes with high authority scores are strongly influenced by others (receivers), and high hub scoring nodes are the influencers (transmitters).

Table 8 sets out the numerical summary of the centrality ranking of the markets according to hub and authority scores. Focusing on the BG-SEMX column presents a realistic view of interconnectedness between the markets, not limited to the interaction of the markets alone but incorporating exogenous variables.

		BG-SEM	**BG-SEMX**	**Lasso-SEM**	**Lasso-SEMX**
		Hub Centrality : Top Three Transmitters			
2015–2017	1	CNOR (0.922)	CSUD (0.842)	CSUD (0.995)	CSUD (0.995)
	2	CSUD (0.387)	CNOR (0.333)	NORD (0.103)	NORD (0.099)
	3	SUD (0.027)	SUD (0.315)	SUD (0.009)	SUD (0.009)
2018–2019	1	CSUD (0.859)	SARD (0.801)	CSUD (0.983)	CSUD (0.984)
	2	CNOR (0.507)	SUD (0.394)	NORD (0.17)	NORD (0.162)
	3	SARD (0.071)	NORD (0.344)	CNOR (0.048)	SARD (0.058)
		Authority Centrality : Top Three Receivers			
2015–2017	1	NORD (0.855)	CNOR (0.571)	CNOR (0.585)	SUD (0.589)
	2	SARD (0.346)	SARD (0.566)	SUD (0.580)	SARD (0.572)
	3	SUD (0.282)	SUD (0.519)	SARD (0.567)	CNOR (0.570)
2018–2019	1	SUD (0.677)	CSUD (0.713)	SARD (0.699)	SARD (0.687)
	2	NORD (0.505)	CNOR (0.506)	SUD (0.556)	SUD (0.580)
	3	CNOR (0.455)	NORD (0.365)	CNOR (0.446)	CNOR (0.435)

Table 8: Centrality ranking of zones according to hub and authority scores for intra-day networks.

The table shows the top three zones central to transmitting risk (according to the BG-SEMX), which are CSUD, CNOR, and SUD for 2015-2017, and SARD, SUD, and NORD for 2018-2019. For sub-period 2015-2017, CSUD and SUD are in the top three of all four competing methods, albeit with different rankings, while CNOR is in two of the four competing methods. For the second sub-period, SARD and NORD are among the top-ranked zones in three of the four networks.

Authority centrality shows that in the event of a major shock to a zone or group of zones, the physical zones most affected are CNOR, SARD and SUD during the 2015-2017 sub-period, while CSUD, CNOR and NORD are the most affected during the 2018- 2019 period. Including

[13] See Borgatti (2005) for details on network centrality measures.

to the ranking of competing methods shows that, during the 2015-2017 sub-period, CNOR, SARD and SUD are the top three risk receivers in at least three of the four methods. For the second period, CNOR makes the list for all four methods, while NORD is ranked highly in two of the four methods.

Overall, we find evidence that intra-day volatility spill-overs in the Italian energy market during the 2015-2017 sub-period spread from CSUD, CNOR, and SUD, while in the 2018-2019 sub-period, they spread from SARD, SUD, and NORD to other zones. The other central zones on the receiving side of intra-day volatility spill-overs are CNOR, SARD and SUD (in 2015-2017), and CSUD, CNOR and NORD (in 2018-2019).

5.3. Inter-day volatility connections

This section illustrates the results of inter-day (or across-day) volatility channels in the physical zones of the market. We begin by selecting the appropriate lag of the VAR and VARX via a BIC for different lag orders ($p \in \{1, \ldots, 7\}$). Table 9 shows the BIC scores corresponding to the different lag orders. The minimum BIC score selects $p = 1$ as the optimal lag order to model inter-day volatility interconnectedness.

	p=1	p=2	p=3	p=4	p=5	p=6	p=7
VAR	**-8.46**	-8.06	-7.61	-7.17	-6.72	-6.34	-5.98
VARX	**-7.95**	-7.57	-7.17	-6.75	-6.30	-5.97	-5.59

Table 9: BIC scores for lag order selection. Boldface values indicate the minimum BIC.

Using the selected lag order, we carry out the yearly rolling window estimation for the Bayesian Graphical (BG) and the Lasso-VAR and VARX. To clarify, the VAR models the across-time lead-lag relationship between log price volatilities. The VARX = VAR + X, where X = exogenous factors (actual/forecast electricity demand and forecast wind generation).

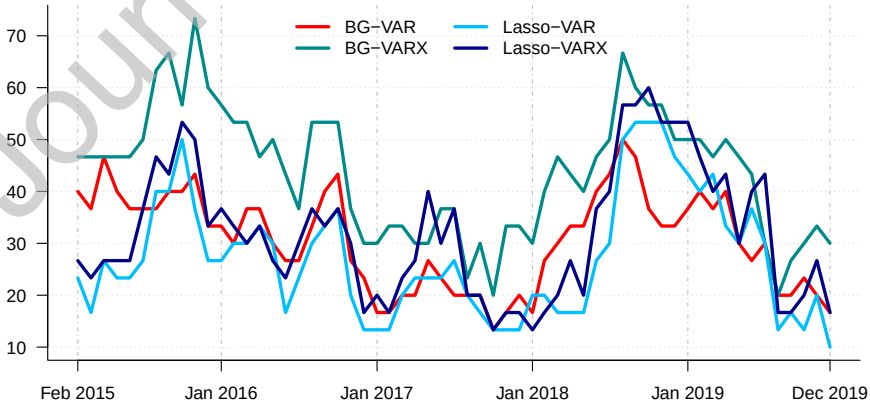

Figure 9: Yearly rolling series of network density from the BG-VAR & VARX and Lasso-VAR & VARX.

The across-day analysis of the network topology is carried out via rolling-window inter-day volatility connectedness in the sample period by comparing networks estimated from BG-VAR, BG-VARX, Lasso-VAR, Lasso-VARX, i.e. with and without exogenous variables. In this paradigm, we estimate the rolling-window network for all four models between March

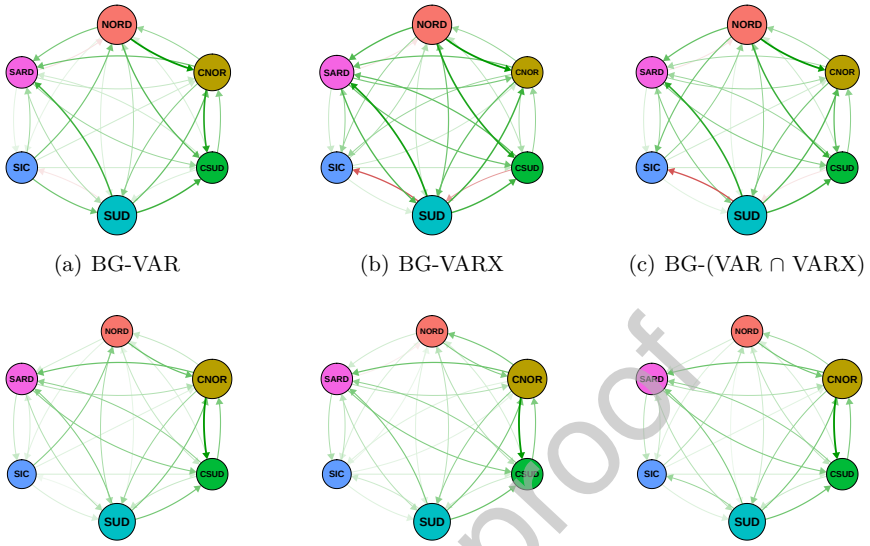

(a) BG-VAR (b) BG-VARX (c) BG-(VAR ∩ VARX)

(d) Lasso-VAR (e) Lasso-VARX (f) Lasso-(VAR ∩ VARX)

Figure 10: **Averaged Inter-day Networks 2015–2017**. Dark (light) green-links indicate strong (mild) positive impacts, and dark (light) red-links for strong (mild) negative effects. The node size is based on hub scores.

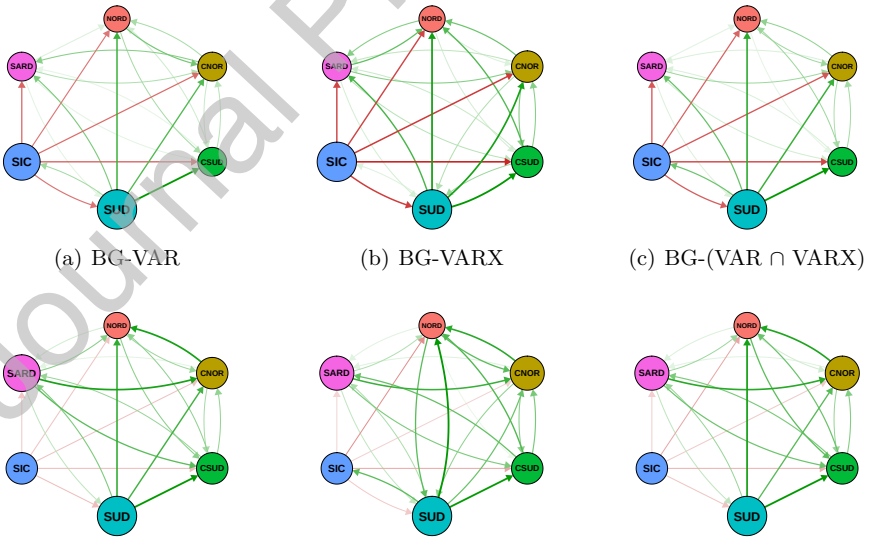

(a) BG-VAR (b) BG-VARX (c) BG-(VAR ∩ VARX)

(d) Lasso-VAR (e) Lasso-VARX (f) Lasso-(VAR ∩ VARX)

Figure 11: **Averaged Inter-day Networks 2018–2019**. Dark (light) green-links indicate strong (mild) positive impacts, and dark (light) red-links for strong (mild) negative effects. The node size is based on hub scores.

2015 and December 2019, which enables us to investigate the impact of electricity demand and the contribution of renewable energy sources (in our case wind) on inter-day volatility connectivity between zones in the last five years (2015-2019). Figure 9 plots network densities

over the period March 2015 to December 2019. Network density peaks can be observed in the period around the last quarter of 2015, 2016, with a mild peak around mid-2017, and the last quarters of 2018 and 2019. Conversely, troughs occur in the second quarter of 2015, mid-2016, Q1 in 2017 and a relatively lengthy trough from Q4 2016 until Q2 in 2018, followed by one from Q4 2018 until Q1 2019 and finally in Q3 2019. One feature is that all four models, namely the BG-VAR, BG-VARX, the Lasso-VAR and Lasso-VARX have similar patterns in the evolution of network densities.

Period	Method	VAR	VARX	VAR ∩ VARX
2015–2017	BG	28	29	28
	Lasso	27	29	27
2018–2019	BG	22	25	22
	Lasso	22	25	22

Table 10: Total number of links in inter-day sub-period networks of the competing methods.

		BG-VAR	**BG-VARX**	**Lasso-VAR**	**Lasso-VARX**
		Hub Centrality : Top Three Transmitters			
2015–2017	1	SUD (0.583)	NORD (0.604)	CNOR (0.664)	CNOR (0.690)
	2	NORD (0.566)	SUD (0.593)	SUD (0.501)	SUD (0.513)
	3	CNOR (0.473)	SARD (0.341)	SARD (0.317)	SARD (0.290)
2018–2019	1	SUD (0.742)	SUD (0.664)	SUD (0.706)	SUD (0.706)
	2	SIC (0.618)	SIC (0.628)	SARD (0.523)	CNOR (0.395)
	3	CNOR (0.161)	CSUD (0.258)	CNOR (0.352)	SARD (0.393)
		Authority Centrality : Top Three Receivers			
2015–2017	1	CSUD (0.628)	CNOR (0.575)	CSUD (0.697)	CSUD (0.688)
	2	SARD (0.527)	CSUD (0.531)	SARD (0.494)	SARD (0.486)
	3	CNOR (0.506)	SARD (0.515)	CNOR (0.418)	CNOR (0.360)
2018–2019	1	CSUD (0.590)	NORD (0.534)	NORD (0.596)	NORD (0.695)
	2	NORD (0.497)	CSUD (0.522)	CSUD (0.561)	CSUD (0.541)
	3	CNOR (0.472)	CNOR (0.492)	CNOR (0.528)	CNOR (0.436)

Table 11: Centrality ranking of zones according to hub and authority score from inter-day networks.

5.4. Comparing Model Performance

As discussed above, BG-SEM(X) infers directed-acyclic-graphs that are suitable for making causal inferences, while the Lasso-SEM estimates networks with bi-directed links. Thus, comparing the performance of the BG-SEM(X) against the Lasso-SEM(X) may not reveal explanatory power of the former since, by construction, the two approaches capture different network structures of the data. The above problem does not occur when comparing the BG-VAR(X) with the Lasso-VAR(X), since both models estimate a Granger-causality type of network where links are directed from lagged variable to current variables and there are no bi-directions.

We compare the performance of the competing methods by computing the network marginal likelihood for the in-sample and out-of-sample predictive exercise to investigate how well the

Bayesian graphical approach fits the data against the Lasso model (see Table 12). We evaluate the out-of-sample performance in terms of the root mean square forecast error (RMSFE) and the predictive marginal likelihood. We perform the out-of-sample prediction via a multi-period forecasting of one month ahead. Since it is well known that VAR models perform better out-of-sample, due to the autoregressive structure of the model, it makes it easier to use past observations to forecast future realizations. Thus, we compare the out-of-sample performance of the models between the BG-VAR and BG-VARX with their Lasso counterparts.

Intra-day Models				Inter-day Models			
BG		Lasso		BG		Lasso	
SEM	SEMX	SEM	SEMX	VAR	VARX	VAR	VARX
Network Marginal Likelihood Score							
-7.2569	-6.9646	-6.8760	**-6.7594**	-7.6190	**-7.5579**	-7.6390	-7.5582
(0.4030)	(0.2965)	(0.1451)	(0.1322)	(0.2218)	(0.1994)	(0.2306)	(0.2136)
Out-of-Sample RMSFE							
-	-	-	-	0.4663	**0.4630**	0.4697	0.5280
-	-	-	-	(0.1031)	(0.1030)	(0.1056)	(0.1063)
Predictive Marginal Likelihood							
-	-	-	-	-6.1972	**-6.1879**	-6.2085	-6.3835
-	-	-	-	(0.3177)	(0.3147)	(0.3261)	(0.3633)

Table 12: Summary statistics of model performance. Bold values indicate the best choice for each metric.

The results in Table 12 show that among the Intra-day estimated models, the Lasso-SEMX records the best and highest score followed by the Lasso-SEM. Among the Intra-day Bayesian graphical models, the BG-SEMX emerged as the best model to fit the contemporaneous causal channels of volatility spillover among the zones. Among the Inter-day estimated models, the BG-VARX reports the best and highest score followed by the Lasso-VARX.

In terms of forecasting performance, the BG-VARX reports the best RMSFE followed by the BG-VAR. The BG-VARX also dominates in terms of the predictive marginal likelihood followed by the BG-VAR.

Thus, we find evidence that models incorporating exogenous macro factors, like actual/forecast electricity demand and forecast wind generation, perform better at fitting the volatility spillover structure in the zonal electricity data. In conclusion, we signal that the choice of the best models depends on the goal of the analysis. Thus, if the interest is to understand the contemporaneous causal directions volatility spillover among the zones, then intra-day BG-SEMX model will be the optimal choice, since it presents an unambiguous direction of influence among the zones. If the purpose of the analysis is to obtain a parsimonious model for forecasting, then the BG-VARX will be the best choice, since it takes advantage of the autoregressive structure of the data.

5.5. Sensitivity Analysis

Several robustness checks were carried out to study the sensitivity of our empirical results using a different measure of price volatility calculated as the median of the absolute deviations

from the median daily price. We construct daily median absolute deviation ($\sigma_{i,t}^{Mad}$), as a measure of outlier-robust realized price volatility, as follows:

$$\sigma_{i,t}^{Mad} = med\ |P_{i,l,t} - \bar{P}_{i,t}|, \qquad l = 1, \ldots, N \tag{9}$$

where $med(A_{i,t})$ is the median value of A_i on day t and N is the total number of hours in a day, i.e., $N = 24$.[14]

The same sub-periods, 2015-2017 and 2018-2019, are used to examine the various scenarios of the network structure. For instance, how does using the standard deviation compare with the use of the median absolute deviation for the various models utilized in the analysis? In other words, how sensitive is our modelling framework to different definitions of volatility? To answer this question, we investigated the above scenarios via within-day and across-day dependencies as illustrated below.

5.5.1. Intra-day Networks

Overall, the results shown in Figures 12 and 13, obtained using the MAD version of the volatility measure, are related and comparable to the risk structures of the findings, using the standard deviation, in Figures 7 and 8, respectively, for the BG and Lasso approaches.

In detail, comparing the different network risk structures in the sub-periods, the results for robust volatility confirm the structures obtained with the standard deviation. There are some small differences in the colors of links and sometimes in the size of nodes. For instance, in the BG-SEMX network 2015-2017 the only red link is from SIC to NORD (Figure 7), while the sole red link is from CSUD to NORD for the same model in the robust framework (Figure 12). Moreover, the node is largest for SARD in the BG-SEMX model 2018-2019 with standard deviation (Figure 8), becoming the largest for NORD in the same model and period, using MAD (Figure 13). The similarity between the two analyses is confirmed by comparing Table 7 to Table 13 which show that the number of network links is very similar in the non-robust and robust case.

In addition, analyzing Table 14 and comparing it with Table 8, shows that the most influential zone in terms of risk transmission underlying almost all models is CSUD for both sub-periods (2015–2017 and 2018–2019) and this confirms the findings of the intra-day analysis based on the standard deviation (Table 8). Moreover, the role of top-transmitter played by NORD - quite clear in the non-robust analysis - is confirmed in the robust analysis (Table 8). CNOR is the zone that is most vulnerable to risk from other zones underlying all models in both sub-periods, confirming the results of the non-robust analysis, as shown in the bottom panel of Table 8. The role of SARD as top-receiver, as seen in the previous analysis, is even stronger with robust volatility in both sub-periods (see Table 14, bottom panel).

5.5.2. Inter-day Networks

The across-day network structures deduced as a result of the BG-VAR/BG-VARX estimated according to the MAD in the sub-period 2015-2017 (Figure 14) are comparable to the structures related to the same models estimated on the standard deviation of prices (Figure 10). In the sub-period 2018-2019, the structures obtained on the MAD (Figure 15) generally have fewer connections between the zones than the networks produced by the same models

[14] As pointed out in section 5.1, the choice of the daily volatility measure affects the final results. In this case, by using the median, we are comparing different hours of the day.

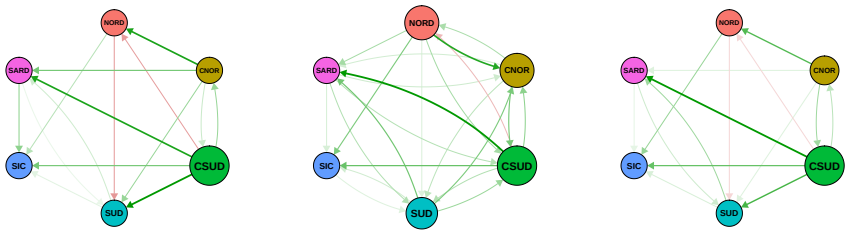

(a) BG-SEM (b) BG-SEMX (c) BG-(SEM ∩ SEMX)

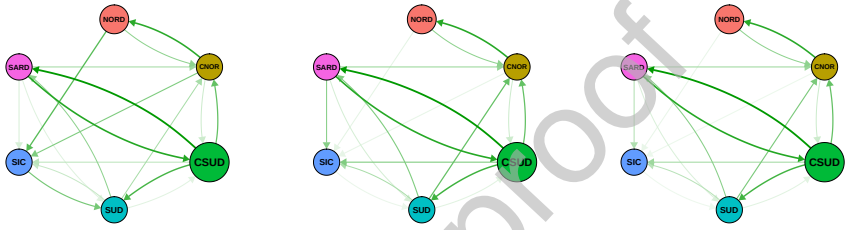

(d) Lasso-SEM (e) Lasso-SEMX (f) Lasso-(SEM ∩ SEMX)

Figure 12: **Averaged Intra-day Networks 2015–2017 - Robust volatility**. Dark (light) green-links indicate strong (mild) positive impacts, and dark (light) red-links for strong (mild) negative effects. The node size is based on hub scores.

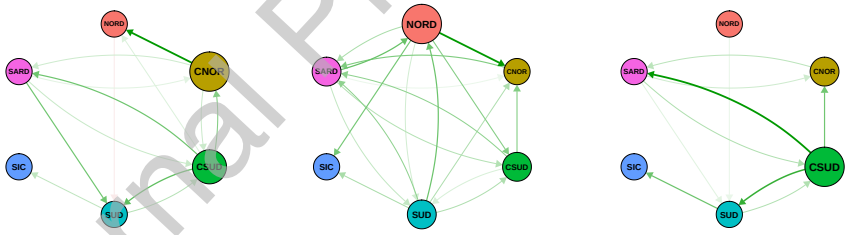

(a) BG-SEM (b) BG-SEMX (c) BG-(SEM ∩ SEMX)

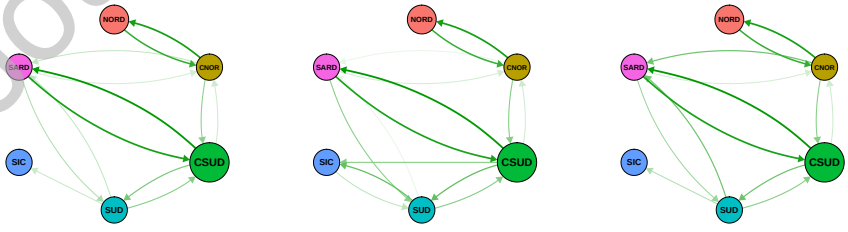

(d) Lasso-SEM (e) Lasso-SEMX (f) Lasso-(SEM ∩ SEMX)

Figure 13: **Averaged Intra-day Networks 2018–2019 - Robust volatility**. Dark (light) green-links indicate strong (mild) positive impacts, and dark (light) red-links for strong (mild) negative effects. The node size is based on hub scores.

using the standard deviation (Figure 11). A striking feature, however, is the fact that, using the standard deviation, the linkages with negative impacts on the network structures are less clear (or absent) in the network topological structures produced using the MAD. This might

Period	Method	SEM	SEMX	SEM ∩ SEMX
2015–2017	BG	15	23	15
	Lasso	18	18	18
2018–2019	BG	13	18	10
	Lasso	13	15	13

Table 13: Total number of links in intra-day sub-period networks of the competing methods. Robust volatility.

		BG-SEM	**BG-SEMX**	**Lasso-SEM**	**Lasso-SEMX**
		Hub Centrality : Top Three Transmitters			
2015–2017	1	CSUD (0.997)	CSUD (0.745)	CSUD (0.988)	CSUD (0.989)
	2	CNOR (0.074)	NORD (0.477)	NORD (0.153)	NORD (0.150)
	3	NORD (0.032)	CNOR (0.400)	SARD (0.015)	SARD (0.019)
2018–2019	1	CNOR (0.867)	NORD (0.941)	CSUD (0.974)	CSUD (0.979)
	2	CSUD (0.497)	SUD (0.277)	NORD (0.217)	NORD (0.183)
	3	SARD (0.032)	SARD (0.141)	SARD (0.070)	SARD (0.085)
		Authority Centrality : Top Three Receivers			
2015–2017	1	SUD (0.710)	SARD (0.737)	SARD (0.710)	SARD (0.702)
	2	SARD (0.639)	CNOR (0.413)	SUD (0.514)	SUD (0.530)
	3	CNOR (0.285)	CSUD (0.406)	CNOR (0.480)	CNOR (0.473)
2018–2019	1	NORD (0.812)	CNOR (0.835)	SARD (0.833)	SARD (0.812)
	2	SARD (0.420)	CSUD (0.503)	SUD (0.451)	SUD (0.509)
	3	SUD (0.295)	SARD (0.198)	CNOR (0.315)	CNOR (0.279)

Table 14: Centrality ranking of zones according to hub and authority score from intra-day networks. Robust volatility.

be due to larger volatilities in the sub-period 2018-2019. These conclusions are confirmed comparing Table 15 to Table 10.

On the whole, in both sub-periods (2015-2017 and 2018-2019) NORD is the zone underlying all four models (BG-VAR/VARX and Lasso-VAR/VARX) with an influential role in the spread of risk to other zones (see Figures 14 and 15 and the corresponding numerical results in Table 16). However, in sub-period 2018–2019, SUD and NORD, with varying rankings, are the zones that transmit the most risk. To sum up, the results in Figures 14 and 15, obtained on the robust volatility, have similar network patterns for the findings in Figures 10 and 11 with the Bayesian graphical approach and the Lasso regularization method applied to the non-robust standard deviation. See Table 16 for their numerical comparison. Again, Table 16, (bottom Panel), shows the top-three risk recipients for sub-periods 2015-2017 and 2018-2019. For instance, SARD is among the top receivers in all the four models BG-VARX and Lasso-VARX with varying rankings in the sub-period 2015-2017. This is not the case in sub-period 2018-2019. In addition, all models are representative of the same zones, i.e. SARD, CSUD, CNOR have the same order of ranking in the two sub-periods. Compared to the non-robust volatility, NORD is the only top risk receiver not confirmed (see Table 11, bottom panel.)

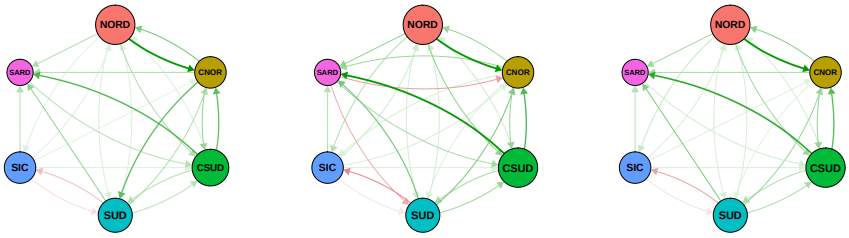

(a) BG-VAR (b) BG-VARX (c) BG-(VAR ∩ VARX)

(d) Lasso-VAR (e) Lasso-VARX (f) Lasso-(VAR ∩ VARX)

Figure 14: **Averaged Inter-day Networks 2015–2017 - Robust volatility**. Dark (light) green-links indicate strong (mild) positive impacts, and dark (light) red-links for strong (mild) negative effects. The node size is based on hub scores.

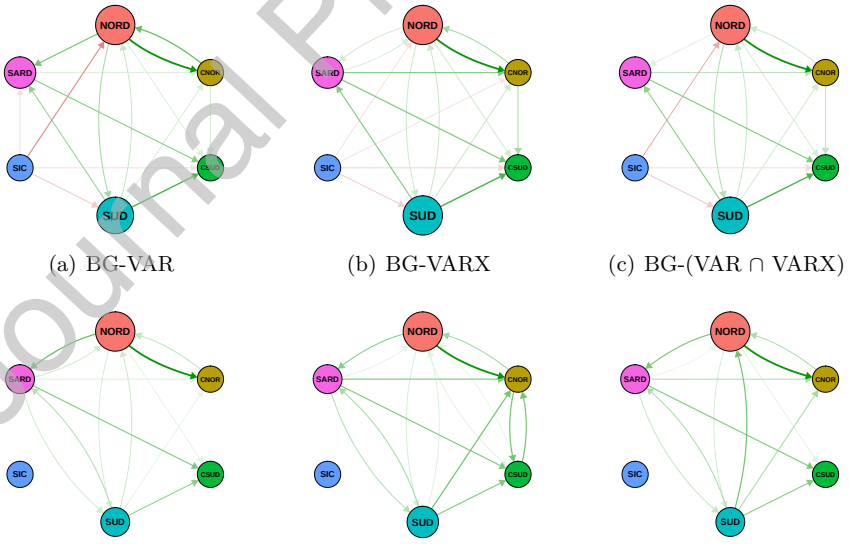

(a) BG-VAR (b) BG-VARX (c) BG-(VAR ∩ VARX)

(d) Lasso-VAR (e) Lasso-VARX (f) Lasso-(VAR ∩ VARX)

Figure 15: **Averaged Inter-day Networks 2018–2019 - Robust volatility**. Dark (light) green-links indicate strong (mild) positive impacts, and dark (light) red-links for strong (mild) negative effects. The node size is based on hub scores.

6. Conclusions

This paper investigates risk propagation between zones in Italy in a period in which the presence of intermittent renewables increased significantly (2015-2019). Bayesian graph-

Period	Method	VAR	VARX	VAR ∩ VARX
2015–2017	BG	24	27	24
	Lasso	23	27	23
2018–2019	BG	16	17	15
	Lasso	13	16	13

Table 15: Total number of links in inter-day sub-period networks of the competing methods. Robust volatility.

		BG-VAR	**BG-VARX**	**Lasso-VAR**	**Lasso-VARX**
		Hub Centrality : Top Three Transmitters			
2015–2017	1	NORD (0.645)	CSUD (0.617)	CSUD (0.858)	CSUD (0.796)
	2	CSUD (0.576)	NORD (0.581)	NORD (0.43)	NORD (0.507)
	3	SUD (0.369)	SUD (0.427)	CNOR (0.216)	SUD (0.257)
2018–2019	1	NORD (0.751)	NORD (0.703)	NORD (0.976)	NORD (0.912)
	2	SUD (0.606)	SUD (0.638)	SUD (0.165)	SUD (0.321)
	3	SARD (0.261)	SARD (0.305)	SARD (0.142)	SARD (0.253)
		Authority Centrality : Top Three Receivers			
2015–2017	1	CNOR (0.711)	CNOR (0.65)	CNOR (0.769)	CNOR (0.825)
	2	SARD (0.574)	SARD (0.643)	SARD (0.525)	SARD (0.441)
	3	CSUD (0.292)	CSUD (0.29)	SUD (0.27)	SUD (0.248)
2018–2019	1	CNOR (0.746)	CNOR (0.688)	CNOR (0.959)	CNOR (0.907)
	2	CSUD (0.585)	CSUD (0.611)	CSUD (0.246)	CSUD (0.381)
	3	SARD (0.287)	SARD (0.364)	SARD (0.136)	SARD (0.171)

Table 16: Centrality ranking of zones according to hub and authority score from inter-day networks. Robust volatility.

ical models are used to estimate how electricity price volatility spreads between the areas into which a zonal electricity market is divided. Specifically, we innovatively use different versions of Bayesian graphical models, with and without exogenous variables, (BG-VAR, BG-VARX, BG-SEM, BG-SEM, BG-SEMX) and compare them to benchmarks (Lasso-SEM and Lasso-SEMX) to investigate risk propagation in the Italian electricity market, accounting for volatility interconnections between zones. One of the most important original contributions of the paper is the disentangling of the analysis into the intra-day and inter-day transmission of risk between zones. Our analysis provides a better understanding of risk transmission. For instance, it is well-known that imbalances of electricity supply and demand due to operational failures, congestions and other causes of shocks such as the presence of more renewable sources in these interconnections are likely to affect the stability and efficiency of the power supply and impact on the volatility of prices. As such, our analysis provides guidance for policymakers to identify zones that can cause these kinds of instability within the electricity system over a day or across days.

In view of this, our approach is to see whether exogenous variables can affect the intra-day and inter-day spreading of risk among zones. Within this framework, we identified and quantified zones that are major transmitters of risk and zones that are vulnerable to volatility spill-overs within a day and over different days, according to the BG-SEMX and BG-VARX, respectively. Considering all summary tables about hub and authority centrality in section 5 and focusing just on the top position of the rankings, we can try to give some synthetic

indications about risk contagion in the Italian zonal electricity market. The top transmitter within the same day is CSUD, because it is at the top in all rankings obtained through the Lasso-SEM and Lasso-SEMX in both sub-periods, using both the standard deviation and the MAD as price volatility measure. Moreover, the score of CSUD is always double than that of the second zone in the same ranking. In the case of the BG approach, CSUD is clearly the top transmitter in 2015-2017. The physical connections of CSUD with three other physical zones (CNOR, SUD and SARD) has surely made CSUD the most important hub for the transmission of risk to the whole system.

In sub-period 2018-2019 CSUD is not even among the three top-transmitters when exogenous variables are included, considering both the standard deviation and the MAD as volatility measures. This means that in the second sub-period, the unidirectional nature of the BG combined with the influence of regressors has changed the contagion structure in the market. SARD and NORD become the top-transmitters, with standard deviation and MAD, respectively. A possible explanation could be the strong increase of wind and hydroelectric generation observed in 2019, particularly in the Northern regions (hydro) and in Sardinia (wind). On the other hand, the most important receiver in the intra-day analysis is SARD, which is the top-receiver in all the rankings obtained using the MAD of prices in the Lasso estimation (with and without regressors) in both sub-periods. According to the robust SEM approach (based on MAD) SARD is the top-receiver in the first sub-period with regressors, but is always among the three-top receivers also in the remaining cases. Another important risk receiver is CNOR, which is at the top of the ranking two times in the BG approach (one in the first sub-period and one in the second) and in both Lasso models based on the standard deviation in the sub-period 2015-2017. Moving to the inter-day analysis, two zones can be identified as top-transmitters: NORD and SUD. The main difference between the two zones is that SUD is the most selected in the rankings of models relying on the standard deviation as measure of price volatility in both sub-periods and with or without external regressors, while NORD is the main top-transmitter when MAD is used. However, SUD is always between the three top-transmitters, even when MAD is used, meaning that the presence of spikes in hourly data for SUD plays a strong influence on the final results. Recalling that CSUD is the top-transmitter in the within-day analysis, we can conclude that the role of main transmitter is passed to the SUD zone when a one-day lag is considered in the connection between physical zones. Therefore, the SUD and CSUD zones play a big role in the spread of volatility in the Italian zonal market. Finally, it is worth stressing the identification of the CNOR as the top receiver in the inter-day analysis: this zone is always the first of the rankings when the MAD is used as measure of price volatility and replaces SARD as top-receiver moving from intra- to inter-day analysis.

Our findings are relevant for policy in terms of market monitoring at the intra-day and inter-day level and require policymakers to pay close attention to these interdependencies. We empirically analyze the sparse interconnectedness of the Italian zonal electricity market to clearly identify the significant channels of relevant potential risk spill-overs and thus build up full picture of risk transmission in the system. Analyzing the zonal market provides useful insights for power generation companies and transmitters in Italy, with implications for markets such as commodities and other financial markets. Furthermore, these findings are relevant for policymakers because they can be used to view and quantify the extent of risk exposure and the spread of systemic risk in the zonal market. They also establish a platform to identify the spread of systemic risk providing a support mechanism for the design of optimal environmental and energy policies by prudently including early-warning and local investment

signals. Similarly, they are useful for risk managers and other practitioners in their efforts to anticipate and prepare for shocks in the electricity market increasing its resilience. Finally, given this amount of information, market participants are able to take prudent decisions in their trading and dealings in the zonal electricity market. In this light, our analysis could be extended to modeling other segmented commodity markets.

For example, it is clear that the CSUD zone is the top-transmitter of risk within the same day, so investments supporting the transmission grid for this zone could be beneficial not only for the Central South, but also for the entire Italian market, reducing price volatility. Conversely, zones receiving risk from zones where intermittent renewable plants are installed (for example SARD) might claim for re-balancing investments in their area. The results obtained suggest that the maximum lag for the spreading of risk is one day. This could be interpreted as a sign of low persistence in the spread of risk which usually disappears within 24 hours. However, when the inter-day network and the intra-day network are compared some differences are evident. For example, we have seen that CSUD is substituted by SUD as top transmitter in the inter-day models, while SARD is replaced by CNOR as top receiver of risk. Market signals could induce the efficient use of transmission grids in order to capture most of the economic benefits from proper congestion management and promote effective network utilization. This indicates that network analysis and its application to systemic risk is a promising tool, providing a platform to meet current and future challenges and solutions to the problems of society and emerging risk. It may also indicate the peak and end of crises. For instance, linkages between the spread of systemic risk in energy systems and the presence of renewable energy sources are extremely significant, especially in the effort to create a single European electricity market, incorporating bidding zones.

Acknowledgments

The authors wish to thank the Associate Editor and four anonymous reviewers for carefully reading the submitted manuscript and for their extremely helpful comments. The authors believe that the suggestions made by the Associate Editor and the reviewers have contributed to the improvement of the paper. However, possible mistakes contained in the current version of the paper must be exclusively attributed to the authors. Emmanuel S. Fianu is grateful (i) for the financial support under grant 01LA1104A from (i) the German Federal Ministry of Education and Research, (ii) to the committee in charge of the Young investigator Training Program (YITP) Research Prizes for Energy Finance Italia 3, and (iii) to the ACRI – Associazione di Fondazioni e Casse di Risparmio Spa, for providing the funding. In addition, many thanks also go to the conference participants of the Energy Finance conference III and the The Center for Quantitative Risk Analysis (CEQURA) conference 2020 for stimulating discussions and comments. In addition, Luigi Grossi acknowledges the financial support from the Italian Ministry of Education and University (MIUR: Ministero dell'Istruzione, dell'Università e della Ricerca), award code FFABR 2017.

References

Acemoglu, D., A. Ozdaglar, and A. Tahbaz-Salehi (2015). Systemic Risk and Stability in Financial Networks. *American Economic Review 105*(2), 564–608.

Ahelegbey, D. F. (2016). The Econometrics of Bayesian Graphical Models: A Review With Financial Application. *Journal of Network Theory in Finance 2*(2), 1–33.

Ahelegbey, D. F., M. Billio, and R. Casarin (2016a). Bayesian Graphical Models for Structural Vector Autoregressive Processes. *Journal of Applied Econometrics 31*(2), 357–386.

Ahelegbey, D. F., M. Billio, and R. Casarin (2016b). Sparse Graphical Vector Autoregression: A Bayesian Approach. *Annals of Economics and Statistics 123/124*, 333–361.

Ahelegbey, D. F. and P. Giudici (2014). Bayesian Selection of Systemic Risk Networks. *Advances in Econometrics: Bayesian Model Comparison 34*, 117–153.

Bertsch, J., T. Brown, S. Hagspiel, and L. Just (2017). The relevance of grid expansion under zonal markets. *The Energy Journal 38*(5), 129–153.

Bigerna, S. and C. A. Bollino (2016). Ramsey Prices in the Italian Electricity Market. *Energy Policy 88*, 603–612.

Bigerna, S., C. A. Bollino, D. Ciferri, and P. Polinori (2017). Renewables diffusion and contagion effect in Italian regional electricity markets: Assessment and policy implications. *Renewable and Sustainable Energy Reviews 68*, 199–211.

Billio, M., M. Getmansky, A. W. Lo, and L. Pelizzon (2012). Econometric Measures of Connectedness and Systemic Risk in the Finance and Insurance Sectors. *Journal of Financial Economics 104*(3), 535 – 559.

Boffa, F., V. Pingali, and D. Vannoni (2010). Increasing Market Interconnection: An Analysis of the Italian Electricity Spot Market. *International Journal of Industrial Organization 28*(3), 311–322.

Bollino, C. A., D. Ciferri, and P. Polinori (2012). Contagion in Electricity Markets: Empirical Evidences from Italian Markets. In *Electricity Markets and Reforms in Europe (Uvalic M., Ed.)*, pp. 49–59. FrancoAngeli.

Borgatti, S. P. (2005). Centrality and Network Flow. *Social networks 27*(1), 55–71.

Caldana, R., G. Fusai, and A. Roncoroni (2017). Electricity forward curves with thin granularity: Theory and empirical evidence in the hourly EPEX spot market. *European Journal of Operational Research 261*(2), 715 – 734.

Cappers, P., J. MacDonald, C. Goldman, and O. Ma (2013). An Assessment of Market and Policy Barriers for Demand Response Providing Ancillary Services in US Electricity Markets. *Energy Policy 62*, 1031–1039.

Ciferri, D., M. C. D'Errico, and P. Polinori (2020). Integration and convergence in European electricity markets. *Economia Politica: Journal of Analytical and Institutional Economics 37*, 463–492.

Creti, A. and F. Fontini (2019). *Economics of Electricity: Markets, Competition and Rules*. Cambridge University Press.

Creti, A., E. Fumagalli, and E. Fumagalli (2010). Integration of Electricity Markets in Europe: Relevant Issues for Italy. *Energy Policy 38*(11), 6966–6976.

de Menezes, L. M. and M. A. Houllier (2015). Germany's nuclear power plant closures and the integration of electricity markets in europe. *Energy Policy 85*, 357–368.

Diebold, F. and K. Yilmaz (2014). On the Network Topology of Variance Decompositions: Measuring the Connectedness of Financial Firms. *Journal of Econometrics 182*(1), 119–134.

Fianu, E. S. (2015). Portfolio Optimization in Zonal Energy Markets: Evidence from Italy. *International Journal of Energy and Statistics 3*(2), 1550006.

Geiger, D. and D. Heckerman (2002). Parameter Priors for Directed Acyclic Graphical Models and the Characterization of Several Probability Distributions. *Annals of Statistics 30*(5), 1412–1440.

Gelman, A. and D. B. Rubin (1992). Inference from Iterative Simulation Using Multiple Sequences, (with discussion). *Statistical Science 7*, 457–511.

Gianfreda, A. and L. Grossi (2012). Forecasting italian electricity zonal prices with exogenous variables. *Energy Economics 34*(6), 2228–2239.

Graf, C., F. Quaglia, and F. A. Wolak (2020, May). Simplified electricity market models with significant intermittent renewable capacity: Evidence from Italy. Working Paper 27262, National Bureau of Economic Research.

Granger, C. W. J. (1969). Investigating Causal Relations by Econometric Models and Cross-spectral Methods. *Econometrica 37*(3), 424–438.

Grossi, L. and F. Nan (2019). Robust forecasting of electricity prices: Simulations, models and the impact of renewable sources. *Technological Forecasting and Social Change 141*, 305 – 318.

Gugler, K., A. Haxhimusa, and M. Liebensteiner (2018). Integration of european electricity markets: Evidence from spot prices. *The Energy Journal 39*(Special Issue 2), 41–67.

Klos, M., K. Wawrzyniak, and M. Jakubek (2015). Decomposition of Power Flow Used for Optimizing Zonal Configurations of Energy Market. In *European Energy Market, 2015 International Conference*, pp. 1–5. IEEE.

Lamadrid, A. J. and T. Mount (2012). Ancillary Services in Systems with High Penetrations of Renewable Energy Sources, The Case of Ramping. *Energy Economics 34*(6), 1959–1971.

Lautier, D. and F. Raynaud (2012). Systemic Risk in Energy Derivative Markets: A Graph-Theory Analysis. *Energy Journal 33*(6), 215–239.

Lisi, F. and E. Edoli (2018). Analyzing and Forecasting Zonal Imbalance Signs in the Italian Electricity Market. *The Energy Journal 39*(5), 1–19.

Pham, T. (2019). Do German renewable energy resources affect prices and mitigate market power in the French electricity market ? *Applied Economics 51*(54), 5829–5842.

Pierret, D. (2013). The Systemic Risk of Energy Markets. Working paper, Université Catholique de Louvain, Center for Operations Research and Econometrics (CORE).

Sapio, A. (2019). Greener, more integrated, and less volatile? A quantile regression analysis of Italian wholesale electricity prices. *Energy Policy 126*, 452 – 469.

Sapio, A. and N. Spagnolo (2016). Price regimes in an energy island: Tacit collusion vs. cost and network explanations. *Energy Economics 55*, 157 – 172.

Sapio, A. and N. Spagnolo (2020). The effect of a new power cable on energy prices volatility spillovers. *Energy Policy 144*, 111488.

Schwartz, D. L. (2012). *The Energy Regulation and Markets Review*. The Law Business Research Limited.

Tibshirani, R. (1996). Regression Shrinkage and Selection via the LASSO. *Journal of the Royal Statistical Society. Series B (Methodological) 58*(1), 267–288.

Trueck, S. and R. Weron (2016). Convenience yields and risk premiums in the EU-ETS. Evidence from the Kyoto commitment period. *Journal of Futures Markets 36*(6), 587–611.

Weron, R. (2000). Energy price risk management. *Physica A: Statistical Mechanics and its Applications 285*(1), 127–134.

Weron, R. (2014). Electricity price forecasting: A review of the state-of-the-art with a look into the future. *International Journal of Forecasting 30*(4), 1030 – 1081.

Wozabal, D., C. Graf, and D. Hirschmann (2016). The effect of intermittent renewables on the electricity price variance. *OR Spectrum 38*, 687–709.

Zugno, M. and A. J. Conejo (2015). A robust optimization approach to energy and reserve dispatch in electricity markets. *European Journal of Operational Research 247*(2), 659 – 671.

Appendix A. Network Sampling Algorithms

The Bayesian inference of a network graph underlying a system of linear equations is made feasible by integrating other parameters analytically to obtain a marginal likelihood function over graphs (see Ahelegbey et al., 2016a; Geiger and Heckerman, 2002). Let $V_y = (y_i, \ldots, y_n)$ be the vector of indices of response variables, and $V_x = (x_1, \ldots, x_q)$ the indices of the predictor variables in X. The network relationship from $x_\psi \in V_x$ to $y_i \in V_y$ can be represented by $(G_{y_i,x_\psi} = 1)$. Following Geiger and Heckerman (2002), the closed-form expression of the local marginal likelihood is given by

$$P(Y|G_{y_i,x_\psi}) = \frac{\pi^{-\frac{1}{2}N}\ \nu_0^{\frac{1}{2}\nu_0}}{\nu_n^{\frac{1}{2}\nu_n}} \frac{\Gamma\left(\frac{\nu_0+T-n_r}{2}\right)}{\Gamma\left(\frac{\nu_0-n_r}{2}\right)} \left(\frac{|X'_\psi X_\psi + \nu_0 I_{n_v}|}{|R'_i R_i + \nu_0 I_{n_r}|}\right)^{\frac{1}{2}\nu_n} \tag{A.1}$$

where $\Gamma(\cdot)$ is the gamma function, $R_i = (Y_i, X_\psi)$, I_d is a d-dimensional identity matrix, n_ψ is the number of covariates in X_ψ, $n_r = n_\psi + 1$, $\nu_0 > n_r$ is a degree of freedom hyper-parameter of the prior precision matrix of (Y, X), and $\nu_n = \nu_0 + T$. Equation (A.1) indicates that only the ratio of the posterior sum of squares depends on the data. Thus, we reduce computational time by pre-computing the part of (A.1) that is independent of the data, for different values of $n_r \in [1, m]$ and for fixed $\nu_0 = m + 2$ and T. We also pre-compute the posterior of the full sum of squares matrix and extract the sub-matrices that relate to $\{X_\psi\}$ and $\{(Y_i, X_\psi)\}$. For computational details of the score function (see Ahelegbey et al., 2016a). The algorithm presented for sampling G is a Metropolis-within-Gibbs sampler with random walk proposal distribution (see Algorithm 1 and Algorithm 2).

Algorithm 1 Sampling SEMX Network

Let $X_t = (Y_t', Z_t')'$ be the vector of explanatory variables for the SEMX model.
Set of responses $V_y = (y_1, \ldots, y_n)$ and predictors $V_x = (x_1, \ldots, x_q)$, $V_y \subseteq V_x$
Initialize $G^{(1)} = \emptyset$
for $h = 1$ to Total iterations **do**
    Pick at random $(r_1, \ldots, r_n)$ from permutations of the integers $\{1, \ldots, n\}$
    for $i = 1 : n$ **do**
        Set $\tilde{y}_i = y_{r_i}$, $\tilde{y}_i \in V_y$ and $G^* = G^{(h)}$
        Draw a candidate explanatory variable, $x_k \in V_x \backslash \{\tilde{y}_i\}$
        if $G^*(x_k, \tilde{y}_i) = 1$ **then** set $G^*(x_k, \tilde{y}_i) = 0$
            Add/remove edge; $G^*(\tilde{y}_i, x_k) = 1 - G^*(\tilde{y}_i, x_k)$
            if G^* is acyclic **then** sample $u \sim \mathcal{U}_{(0,1)}$
                Compute $\phi = \exp\,[\, \log P(Y|G_{y_i}^{(*)}) - \log P(Y|G_{y_i}^{(h)}) \,]$
                if $u < \min\{1, \phi\}$ **then** $G^{(h+1)} = G^*$
                else $G^{(h+1)} = G^{(h)}$
            else $G^{(h+1)} = G^{(h)}$

Algorithm 2 Sampling VARX Network

Let $X_t = (Y_{t-1}', \ldots, Y_{t-\hat{p}}', Z_t')'$ be the vector of predictors for the VARX model.
Set of responses $V_y = (y_i, \ldots, y_n)$ and predictors $V_x = (x_1, \ldots, x_q)$
Initialize $G^{(1)} = \emptyset$
for $y_i \in V_y$ **do**
    for $x_j \in V_x$ **do**
        Compute $\phi_a = P(Y|G_{y_i,\emptyset}^{(1)})$ and $\phi_b = P(Y|G_{y_i,x_j}^{(1)})$
        if $\phi_b > \phi_a$ **then** $G_{y_i,x_j}^{(1)} = 1$
        else $G_{y_i,x_j}^{(1)} = 0$

for $h = 2$ to Total iterations **do**
    for $y_i \in V_y$, set $G_{y_i}^{(*)} = G_{y_i}^{(h-1)}$ **do**
        Draw a candidate explanatory variable, $x_k \sim V_x$
        Add/remove link from x_k to y_i: $G_{y_i,x_k}^{(*)} = 1 - G_{y_i,x_k}^{(h-1)}$
        Compute $\phi = \exp\,[\, \log P(Y|G_{y_i}^{(*)}) - \log P(Y|G_{y_i}^{(h-1)}) \,]$.
        Draw $u \sim \mathcal{U}(0, 1)$.
        if $u < \min\{1, \phi\}$ **then** $G_{y_i}^{(h)} = G_{y_i}^{(*)}$
        else $G_{y_i}^{(h)} = G_{y_i}^{(h-1)}$

For the empirical application, we set the hyper-parameters as follows: $\pi_{ij} = 0.5$ (which leads to a uniform prior on the graph space), $\eta = 100, \delta = n + 2$ and $\Lambda_0 = \delta I_n$. We set the number of MCMC iterations to sample 20,000 graphs and ensure that the convergence is tested via the potential scale reduction factor (PSRF) of Gelman and Rubin (1992).

Appendix B. Autocorrelation functions

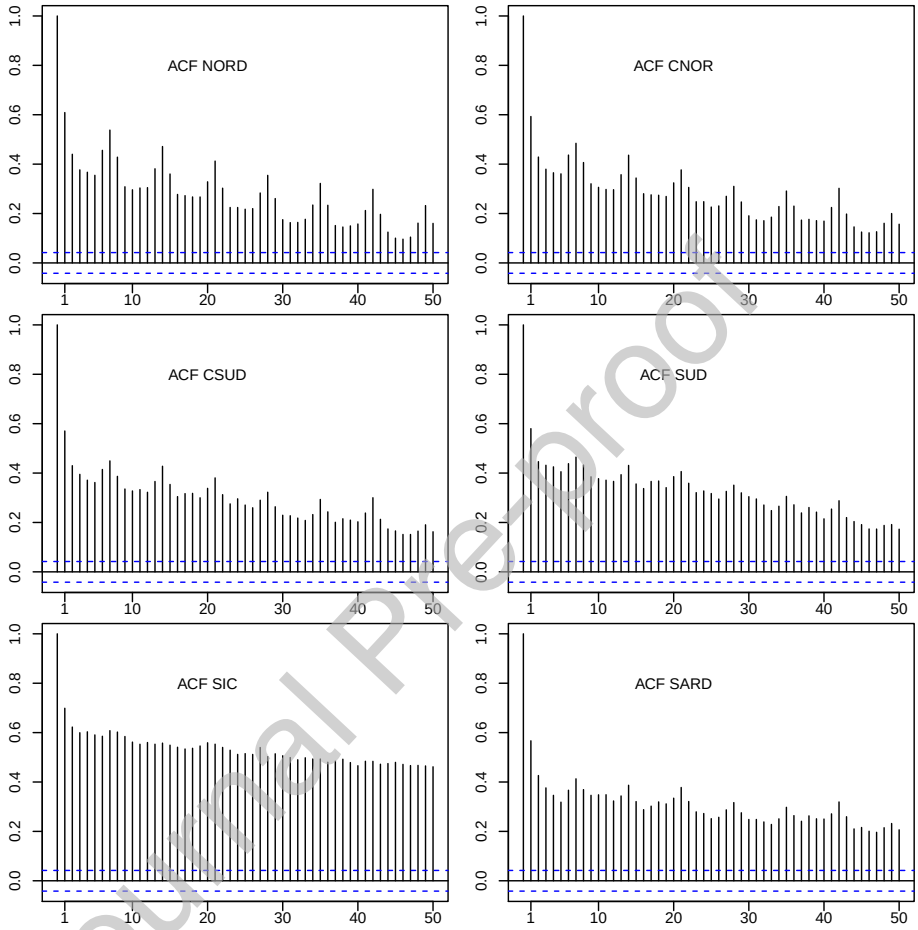

Figure B.1: Autocorrelation functions of the log-volatility (log of standard deviation of prices). Lags are on the x-axis.

.